J. Porphyrins Phthalocyanines Downloaded from www.worldscientific.com
by UNIVERSITY OF NEW ENGLAND on 04/25/20. Re-use and distribution is strictly not permitted, except for Open Access articles.

This is a JAM - Just Accepted Manuscript

Journal of Porphyrins and Phthalocyanines

Article Title: **Development of alkyne-BODIPYs as viscosity sensitive fluorescent probes for enumeration of bacterial cells**

Author(s): **Dijo Prasannan, Suchithra Tharamel Vasu, Chellaiah Arunkumar, Pattiyil Parameswaran**

DOI: **10.1142/S1088424620500194**

To be cited as:

Dijo Prasannan, Suchithra Tharamel Vasu, Chellaiah Arunkumar, Pattiyil Parameswaran, Development of alkyne-BODIPYs as viscosity sensitive fluorescent probes for enumeration of bacterial cells, *Journal of Porphyrins and Phthalocyanines*, doi: 10.1142/S1088424620500194

Received: 17 January 2020
Accepted: 16 April 2020

This is the accepted and unedited version of a newly accepted manuscript after peer-review evaluation. No copyediting, typesetting or proof correction has been performed, so it is by no means the definitive final version of the manuscript. This format allows a rapid display online with a DOI, which means that the manuscript is already citable in a sustainable manner.

It has been uploaded in advance for the benefit of our customers. The manuscript will be copyedited, typeset and proofread before it is released in the final form. As a result, the published copy may differ from the unedited version. Readers should obtain the final version from the above link when it is published. The authors are responsible for the content of this Accepted Article.

When the corrected proof will be available, the manuscript will move to the Online Ready page of the website. The definitive version with page numbers will be available after publication of the issue in which it takes place.

Thanks to this free and optional opportunity, the newly accepted manuscript can be quickly shared with the scientific community.

In no case, WorldScientific can be held responsible of mistakes in the content of use of this Just Accepted Manuscript.

J. Porphyrins Phthalocyanines Downloaded from www.worldscientific.com
by UNIVERSITY OF NEW ENGLAND on 04/25/20. Re-use and distribution is strictly not permitted, except for Open Access articles.

Development of alkyne-BODIPYs as viscosity sensitive fluorescent probes for enumeration of bacterial cells

Dijo Prasannan,[a] Suchithra Tharamel Vasu,[b] Chellaiah Arunkumar[a] and Pattiyil Parameswaran[c]*

[a]*Bioinorganic Materials Research Laboratory, Department of Chemistry, National Institute of Technology Calicut, NIT Campus P.O., Calicut, India-673 601.*
[b]*School of Biotechnology, National Institute of Technology Calicut, NIT Campus P.O., Calicut, India-673 601.*
[c]*Theoretical and Computational Chemistry Laboratory, Department of Chemistry, National Institute of Technology Calicut, NIT Campus P.O., Calicut, India-673 601.*

Abstract

We report a series of alkyne-functionalized *meso*-aryl boron dipyrrin (BODIPY) molecular rotors sensitive to viscosity. The planar and twisted conformation within the molecular structure decides the viscosity dependent behavior. The variations in fluorescence lifetime and intensity were appreciable to the local viscosity. Hence, the dye has been successfully employed in the enumeration of microbes by considering the proportionate fluorescence intensity of the BODIPYs as an index of the number of cells per ml. With increasing cells per mL, the viscosity of the bacterial solution is increased. Consequently, the fluorescent intensity of the sample containing BODIPY tends to increase due to the restricted rotation in the viscous medium. The BODIPY probe offers high sensitivity and is easier than other conventional techniques of colony-forming unit (CFU) determination. The theoretical studies indicate that the intramolecular charge transfer is responsible for the enhanced fluorescence intensity in a high viscous solvent.

Keywords: BODIPY, viscosity, fluorescence, bacterial enumeration, restricted rotation

Introduction

Intracellular viscosity plays an essential role in cellular biophysics (eg., signaling, diffusions of nutrients or metabolites, changes in proteins configurations, etc.), and any subtle alterations are linked to diseases.[1] Accumulation of misfolded proteins in the endoplasmic reticulum during diabetes, increase in mitochondrial viscosity in Alzheimer's disease, reduced viscosity of nucleoplasm with Hutchinson–Gilford progeria syndrome, etc., are some of such biological processes.[2,3] Hence, monitoring real-time viscosity variations is of great importance in biological research as well as clinical diagnoses. *Meso*-substituted BODIPYs involving twisted intramolecular charge transfer (TICT) or Forster resonance energy transfer (FRET) have

ACCEPTED MANUSCRIPT

J. Porphyrins Phthalocyanines Downloaded from www.worldscientific.com
by UNIVERSITY OF NEW ENGLAND on 04/25/20. Re-use and distribution is strictly not permitted, except for Open Access articles.

emerged as fluorescent molecular rotors (FMRs) to probe micro-viscosity of cell domains.[4,5] The rotation of the *meso*-aryl ring and accompanying distortion of the dipyrrin framework hinders free rotation in a viscous medium. This hindered rotation prohibits the non-radiative processes of the electronically excited dyes resulting in increased emission intensity, quantum yield, and lifetime. BODIPY based fluorescent rotors help in monitoring viscosity variations during apoptosis,[6] lipid oxidation, cell lysis in microbes *via* protein or DNA leakage, bacterial sporulation and deactivation, bacterial membrane viscosity changes in response to variations in temperature, identifying tumor on the basis viscosity of normal cells, etc.[5,7–10]

Bacterial enumeration is an important parameter to understand the ecological role of microbes in any environment to determine its rate of growth/ death, particularly in the food and dairy industry. Conventionally, bacterial enumeration has been accomplished *via* serial dilution-viable plate count or turbidometric methods which are time-consuming, and suffer from high variability as well as a limited dynamic range due to self-chemical or microbial action on the substrate.[10] Both clinical analyses and industry demand fast and reliable quantification of bacterial suspensions. Here, we exploit the viscosity sensitive property of a BODIPY compound as a novel method for the enumeration of bacteria. It is based on the fact that the viscosity due to cell density is proportional to the fluorescence characteristics of BODIPY. Hence the proposed method, which is based on the emission properties of BODIPYs, offers a more accurate, quick, and repeatable process in the bacterial enumeration.

Here, *para*- and *meta*-derivatives of three structurally similar fluorescent probes (**1b-6b**) are developed. The restricted rotation is certainly more pronounced in *ortho* derivatives as compared to *meta* and *para* derivatives. However, the effect of *ortho*-substituents is well studied earlier [11] Also, symmetrically substituted FMRs are reported to show a declined viscosity sensing property.[12] Here we have designed structurally asymmetric meta-derivatives, and the effect of structural alterations in the deactivation of the excited state through the non-radiative pathway is investigated theoretically. Since the propargyl groups are susceptible for facile functionalization and precursors group for synthesizing click products, we have selected one of the substituents as the propargyl group (**1b** – **4b**). The practical utility of viscosity sensitive molecules as a novel method for the enumeration of bacteria is also demonstrated using the model organism *Escherichia coli*.

ACCEPTED MANUSCRIPT

J. Porphyrins Phthalocyanines Downloaded from www.worldscientific.com
by UNIVERSITY OF NEW ENGLAND on 04/25/20. Re-use and distribution is strictly not permitted, except for Open Access articles.

Results and discussion

The stepwise synthesis of dipyrromethane precursors and their BODIPYs were afforded by following general procedure.[13,14] The synthetic route employed is outlined in scheme 1. The crude compounds purified by column chromatography afforded *meso*-aryl substituted dipyrromethanes in 30-64 % and *meso*-aryl substituted BODIPY dyes in 56-84 % yield.

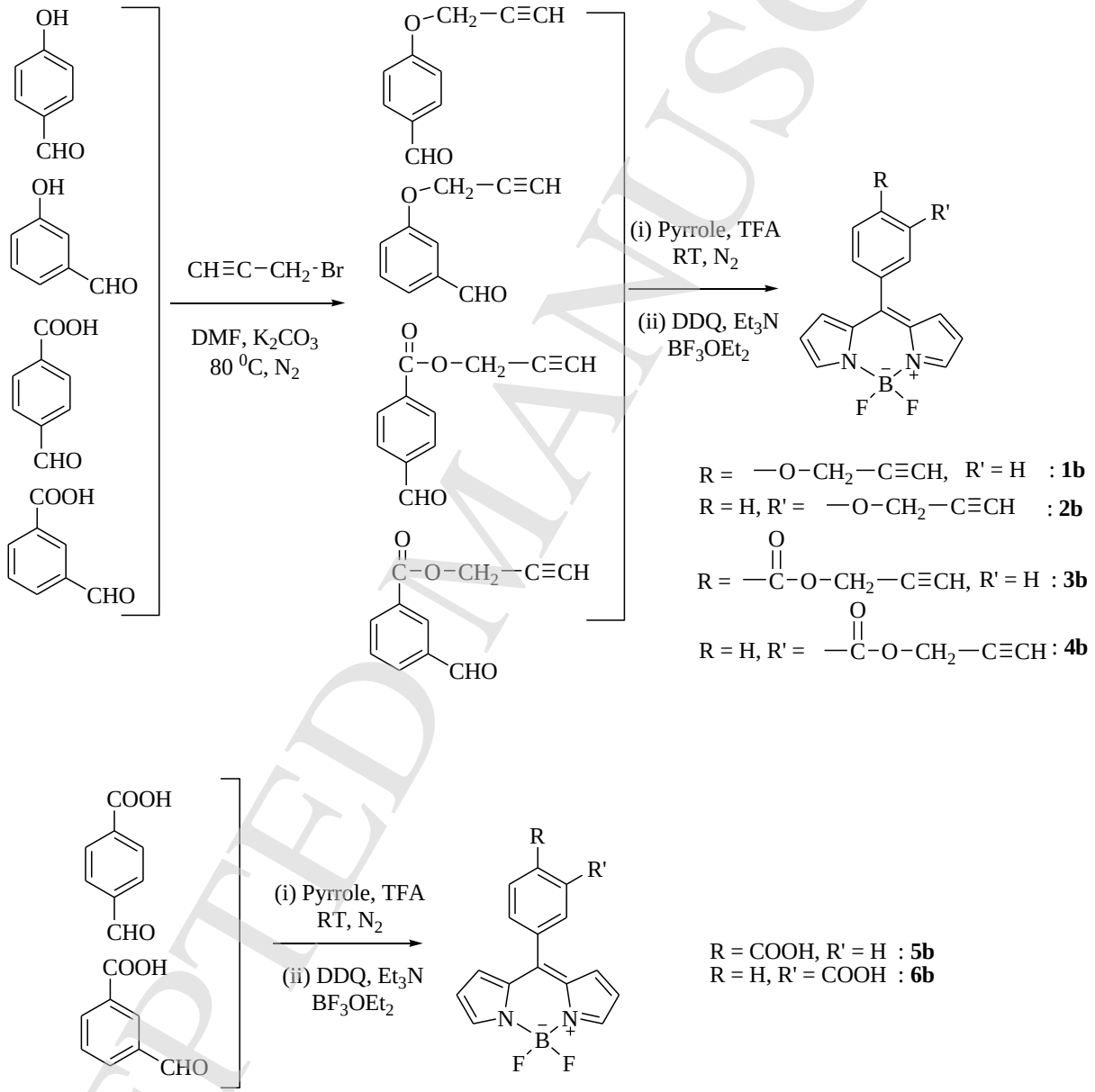

Scheme 1. Synthetic scheme of BODIPYs, **1b-6b**.

ACCEPTED MANUSCRIPT

J. Porphyrins Phthalocyanines Downloaded from www.worldscientific.com
by UNIVERSITY OF NEW ENGLAND on 04/25/20. Re-use and distribution is strictly not permitted, except for Open Access articles.

The integrated intensities of all the proton and carbon signals in ^{1}H and ^{13}C NMR respectively are very well in concordance with the expected structure. The NMR and mass spectra are given in the supplementary information (Figures S1 to S22). The IR spectra of all the BODIPYs showed characteristic -C≡C and terminal alkyne -CH near 2120 and 3400 cm^{-1}, respectively. The aromatic =C-H, -C-H, and Ar-O and stretching frequencies were found at 3100, 2900, and 1263cm^{-1}, respectively. The vibrations corresponding to B-N, B-F, and β-H of pyrrole ring[15] of the BODIPY core appeared in the vicinity of 1534-1414 and 762-781 cm^{-1} respectively.

Single crystal X-ray diffraction studies

The structural characterization of all the compounds was obtained by single-crystal X-ray diffraction analyses. ORTEP diagrams are shown in Figure 1. The packing diagrams, crystal structure parameters, and interactions present in the compounds were shown respectively in Tables S2, S3, and Figure S23.

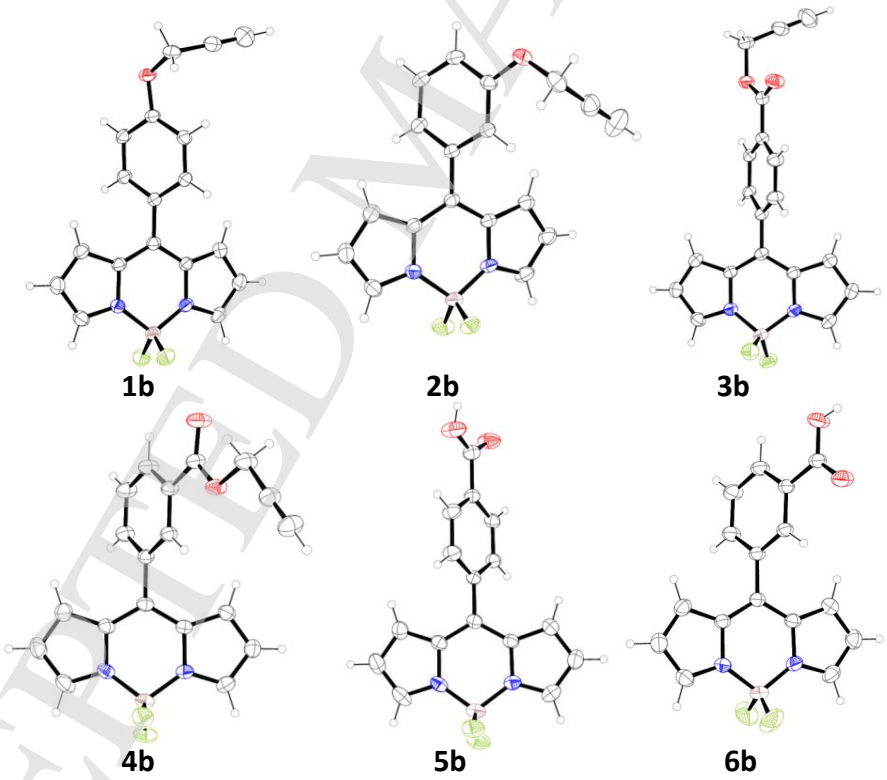

Fig. 1. ORTEP diagrams of compunds **1b - 6b** shown at 40 % probability ellipsoids. (Solvent molecules are omitted for clarity). Atom colors: Gray-Carbon; Blue-Nitrogen; Green-Fluorine; Pink-Boron; White-Hydrogen; Red-Oxygen).

ACCEPTED MANUSCRIPT

J. Porphyrins Phthalocyanines Downloaded from www.worldscientific.com
by UNIVERSITY OF NEW ENGLAND on 04/25/20. Re-use and distribution is strictly not permitted, except for Open Access articles.

Single crystals of suitable diffraction quality of compounds were obtained by a slow evaporation method using a variety of solvents, including chloroform, hexane, methanol, etc. at room temperature for 6-7 days. Compounds, **1b** and **3b,** are crystallized in the monoclinic system, whereas **2b**, **4b, 5b.**DMF and **6b** are crystallized in triclinic.

The bond lengths and bond angles of BODIPY derivatives were similar to those reported previously.[14] The nitrogen atom of two pyrrole units and two fluorine atoms are tetrahedrally coordinated to the boron atom. The B−N and B−F bond distances are in the range of 1.527-1.545 Å and 1.336-1.393 Å, respectively. The F–B–F plane is twisted 86.8-89.8° with respect to the BODIPY core structure. The mean plane displacement of the 12-atoms of BODIPY core deviates from ~0.0262 to ~0.0988 Å, indicating its planar nature. Further, the aryl ring present in the meso-position is oriented perpendicular to the plane of the BODIPY core with the dihedral angle ranging from 52.7-64.4º, which is comparable to the literature values.[14] This indicates that the aromatic ring is non-conjugated to the core structure.

Compounds, **1b,** and **2b** exhibit a similar kind of anti-parallel and herringbone-like structure, as reported previously through various intermolecular interactions (Figure S23a, b; Table S2). The crystal packing of *para*-carboxyl (**5b**) and *para*-alkyne (**3b**) derivatives form a 2D network. BODIPY core is connected through the solvent lattice (DMF) and B···H, F···H, F···C, C···C, H···O interactions in **5b** and **3b,** respectively (Figure S23c, e). The *meta*-carboxyl (**6b**) and *meta*-alkyne (**4b**) derivatives form zig-zag 3D structural arrangements that are connected through exclusively as F···H and C···H interactions (Figure S23d, f).

Photophysical properties

The absorption spectra of BODIPYs show a narrow, strong $S_0 \rightarrow S_1$ transition around 502 nm with a 0-1 vibrational transition as a shoulder at around 480 nm as well as a broad $S_0 \rightarrow S_2$ band around 380 nm. These values are comparable to the structurally similar BODIPY molecules.[14] The mirror shaped emission peak stems from $S_1 \rightarrow S_0$ transition. The peaks appear sharp due to the virtually identical geometries of the ground and excited states in the Franck-Condon region.[2,16] The optical transition from the ground state to the second excited singlet state, centered at 480 nm, is more pronounced due to the reduced splitting between the two states. The steady-state absorption and fluorescence features examined at the different polarities and are summarized in Table S4. The blue shift in absorption with solvents of increasing polarity

ACCEPTED MANUSCRIPT

J. Porphyrins Phthalocyanines Downloaded from www.worldscientific.com
by UNIVERSITY OF NEW ENGLAND on 04/25/20. Re-use and distribution is strictly not permitted, except for Open Access articles.

is explained as the lower electric dipole moment of LUMO as compared to HOMO.[16] The geometry relaxation of BODIPY molecules upon photoexcitation affects the energy levels of molecular orbitals.[15] The geometries of excited states of S_1 and S_0 of the BODIPY framework being similar, the difference between absorption and the emission energy will be small. The small Stokes' shift between the two bands is thus consistent with the rigid and neutral dipyrrin that hampers major geometrical relaxations at excited state associated with emission broadening.[2]

Fluorescence response to solvent viscosity

Here, we have designed meso-substituted BODIPYs, **1b-6b** with unsubstituted pyrrole rings. For a BODIPY molecular rotor, the alkyl groups usually found on the pyrrole units are excluded because excited-state dynamics are mainly governed by *meso*-phenyl rotation.[12,16] The viscosity and polarity sensitivities are two exclusive properties of FMRs. Hence, those rotors which show solvent-polarity-dependent emission, do not show the FMR property and vice versa.[17] A maximum of 5 nm shift in emission wavelength was observed when the solvent was changed from less viscous ethanol to high viscous glycerol. Glycerol and ethanol are completely miscible and are important in the pharmaceutical industry. Hence we used glycerol-ethanol mixtures as viscosity model. The glycerol-ethanol mixtures as viscosity model has been reported earlier by Muggeridge and co-workers [22]. BODIPYs **1b-6b** are insensitive to the polarity of the solvent and hence be considered as perfect FMRs. The fluorescence intensity of all compounds increases linearly with increasing viscosity at room temperature. While increasing the viscosity from ethanol (1.20 cP) to glycerol (1457 cP), the compounds **1b-6b** exhibited 8-40-fold increase in emission intensity respectively. (Figures 2 and S25-29). The fluorescence quantum yield of BODIPYs also exhibited a linear increase with viscosity.[2] The fluorescence quantum yield decreases with increasing electron-withdrawing nature of the substituent at the *para* position of the phenyl group [18]. However, this effect is very negligible for the compounds **1b-6b**. The fluorescence quantum yield of compounds **1b-6b** in ethanol has an average value of 0.03.

The viscosity dependence of the fluorescence intensity of FMRs is expressed using the Forster–Hoffmann theory as,

$$ln\frac{I}{I_0} = C + xln(\eta)$$

ACCEPTED MANUSCRIPT

J. Porphyrins Phthalocyanines Downloaded from www.worldscientific.com
by UNIVERSITY OF NEW ENGLAND on 04/25/20. Re-use and distribution is strictly not permitted, except for Open Access articles.

where I is the emission intensity, η is the viscosity of the solvent, C is an experimental constant depending on the temperature, and x is the viscosity sensitivity of the rotors.[19] The higher the x value, the more sensitive is the emission intensity of an FMR toward the viscosity variation. The slope of the log(fluorescence intensity) *versus* log (viscosity) plot gives the sensitivity for a rotor. According to Foster and Hoffman, a perfect rotor exhibits a sensitivity of 0.6[19,20] Among the dyes, the best sensitivity was observed for **3b** (0.52) and **4b** (0.50) respectively. As predicted by Forster and Hoffmann, the log-log relationship between viscosity and quantum yield also holds well in all cases (Figure S31).

The internal motions, like the rotation of the aryl substituent and accompanying distortion of the dipyrrin core due to the frictional forces with the surrounding medium, provide an active non-radiative decay channel for the rotors.[7] These changes are reflected in the emission properties with varying viscosity of the solvent. The fluorescence intensity of rotors was found to be less in non-viscous solvents, which are attributed to the free rotation of a *meso*-aryl group of BODIPY.[4] The free rotation about the C≡C bonds in the excited state may cause twisting of molecular configuration. Consequently, the emission appears weak in low viscous solutions. The free rotation of the single bond connecting the *meso*-aryl carbon and oxygen of –O-CH_2-C≡CH in molecular rotors (**1b-4b**) causes the non-radiative decay. As the energy of the excited state is released through non-radiative transitions, the molecules are weakly fluorescent with a quantum yield (Φ_f) ranging from 0.01 to 0.05 in ethanol (Table S8). The rotation through the *meso*-phenyl C-C bond is restricted in the presence of a highly viscous solvent, such as glycerol[4], and the excited energy is reserved for emission without non-radiative energy dissipation. With increasing viscosity, the non-radiative processes caused by configurational relaxation from the planar locally-excited state (S_1^{LE}) to the twisted intramolecular charge transfer excited state (S_1^{TICT}) are suppressed. There arises a restriction in the rotation (or twisting) of phenyl groups with respect to the -O-C bridge of the propargyl group. Subsequently, the radiative emission from S_1^{LE} increases, which in turn reduces the fluorescence efficiencies. Thus, molecular rotors may perceive the local viscosity *via* intramolecular twisting motion that occurs in an excited state.[21] These twisting motions may slow down with increasing viscosity due to which compounds **1b-6b** displays higher emission intensity in 100% glycerol than other mixtures of ethanol/glycerol[22] (FigureS 2 and S25-S29).[2,23] Thus, kinetically-restricted rotation of the phenyl group with respect to the dipyrrin core hampers the non-radiative decay channel.[2]

ACCEPTED MANUSCRIPT

J. Porphyrins Phthalocyanines Downloaded from www.worldscientific.com
by UNIVERSITY OF NEW ENGLAND on 04/25/20. Re-use and distribution is strictly not permitted, except for Open Access articles.

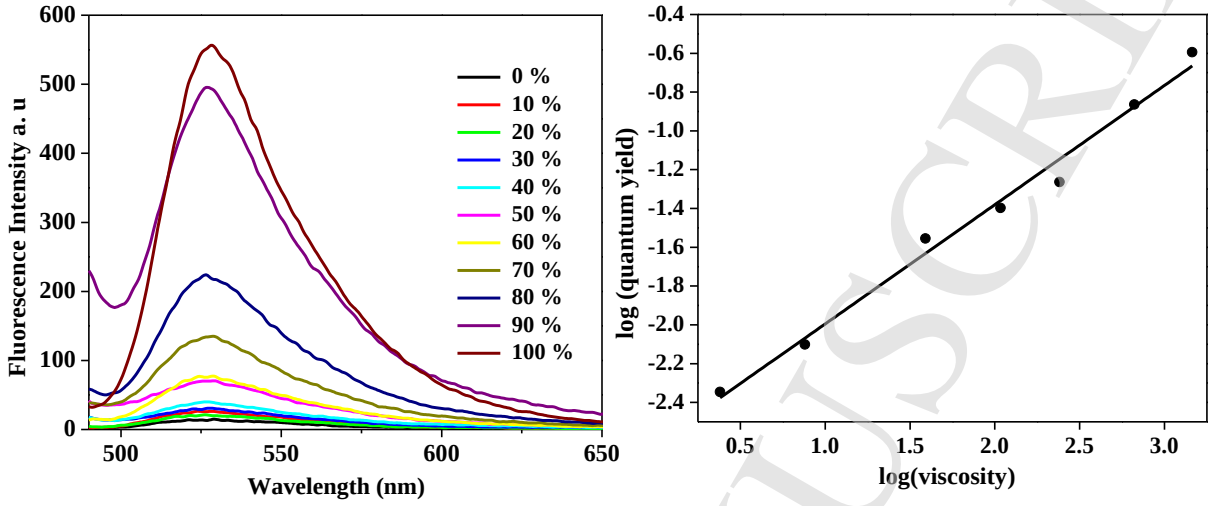

Fig 2. (a) Emission spectra of **3b** in ethanol-glycerol mixtures of different viscosity and (b) log (quantum yield) *vs.* log (viscosity) of **3b**.

The viscosity sensitivity of molecular rotors **3b** and **4b** are comparable to the other classes of benchmark molecular rotors such as homodimeric BODIPYs.[19] The good linear relationship between log (emission intensity) and log (viscosity) with a correlation coefficient of 0.98 indicates that the probes can be used for the quantitative determination of viscosity (Figure S30). Although all the fluorescent probes **1b-6b** described here were found to be sensitive to local viscosity, fluorescence quantum yield of **3b** was greatly enhanced by about 63 fold with when viscosity was increased from ethanol to glycerol. Hence, we advanced further application studies with **3b**.

Fluorescence lifetime analyses

The fluorescence lifetime (τ) of a selected molecular rotor, **3b,** has been determined to get more insight into the variations in local viscosity.[1] The lifetime evaluated in 100% ethanol, 50/50 ethanol/glycerol, and 100% glycerol was best fitted with biexponential function and was observed to be 0.25, 1.96, and 2.49 ns respectively (Figure 3). The fluorescence lifetime was found to increase with increasing viscosity. As Forster–Hoffmann equation is also applicable to the lifetime and viscosity as,[23]

$\ln(\tau) = C_0 + x\ln(\eta)$, where C_0 is constant.

ACCEPTED MANUSCRIPT

J. Porphyrins Phthalocyanines Downloaded from www.worldscientific.com
by UNIVERSITY OF NEW ENGLAND on 04/25/20. Re-use and distribution is strictly not permitted, except for Open Access articles.

This confirms that **3b** as an ideal rotor to monitor intracellular viscosity. A calibration curve of viscosity versus lifetime can be constructed using solvents of different viscosities and subsequently applied to map the viscosity inside the cells. Further, radiative and non-radiative rate constants, K_r and K_{nr}, were calculated from the experimentally measured quantum yields φ_f and the fluorescence lifetime, τ using the following equation,[20]

$$\Phi_f = \frac{k_r}{k_r + k_{nr}} \text{ and } \tau_f = \frac{1}{k_r + k_{nr}}$$

The values of K_r (0.04 to 0.35 ns^{-1}) do not vary with change in viscosity. On the other hand, K_{nr} shows a sharp decrease with increasing viscosity from 4.02 to 0.06 ns^{-1} when solvent changes from ethanol to glycerol. This strongly suggests that the increase in quantum yield with increasing viscosity is principally through the suppression of non-radiative processes.[20]

Figure 4 shows the fluorescence lifetime imaging of BODIPY **3b**, in 100% ethanol, 50/50 ethanol/glycerol, and 100% glycerol, which further reflects the possibility of biological application of the molecule in probing viscosity.

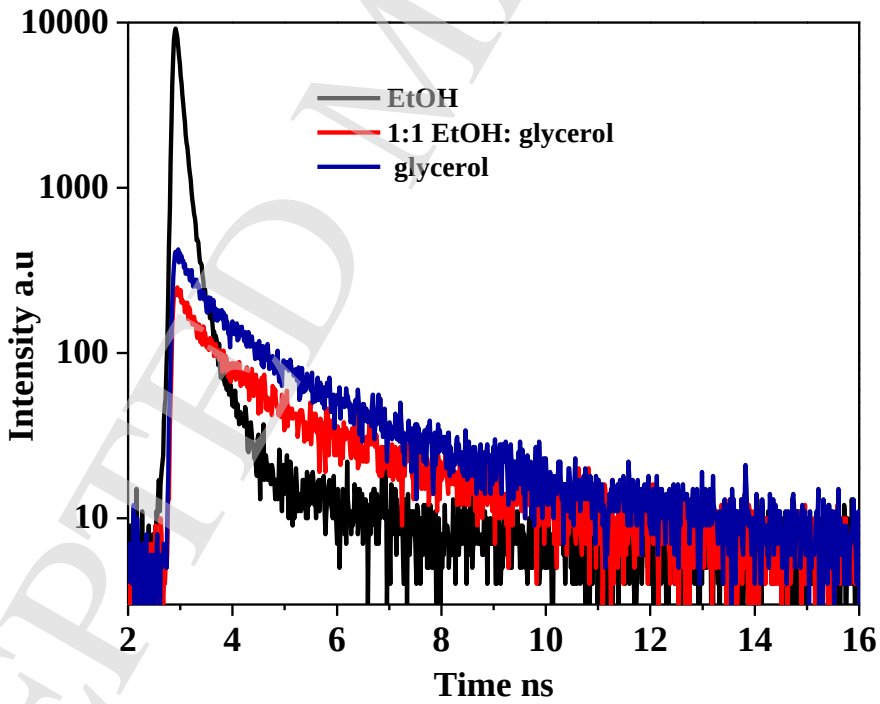

Fig. 3. Fluorescence lifetime of 3b in (a) ethanol, black; (b) 1:1 ethanol:glycerol, red; and (c) glycerol, blue.

ACCEPTED MANUSCRIPT

J. Porphyrins Phthalocyanines Downloaded from www.worldscientific.com
by UNIVERSITY OF NEW ENGLAND on 04/25/20. Re-use and distribution is strictly not permitted, except for Open Access articles.

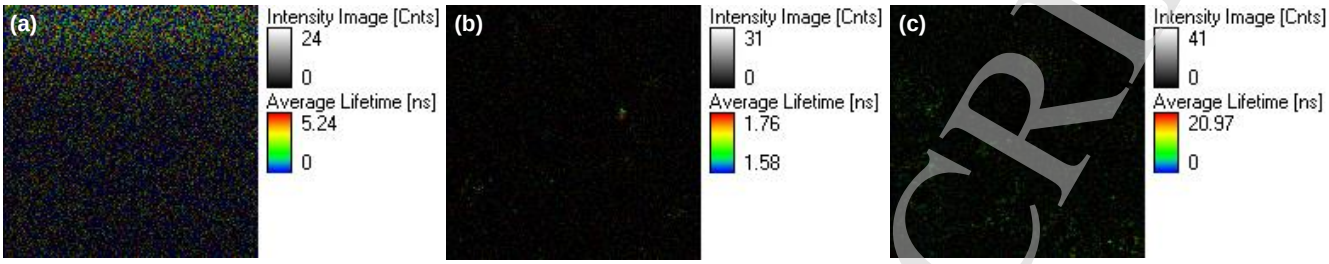

Fig. 4. Fluorescence lifetime imaging of **3b** in (a) ethanol; (b) 1:1 ethanol: glycerol and (c) glycerol.

Theoretical studies

To explore the charge transfer in fluorescent molecular rotors, **1b**-**6b**, TDDFT calculations were performed. Tables S5 and S6 list the lowest-energy transitions and respective oscillator strength at ground state and transition state for the rotation of phenyl ring. The ground-state geometry optimizations were performed by DFT functional BP86[24,25] with Def2-SVP[26] basis set. The single point calculations were performed at the M06[27] level with Def2-TZVPP[28] basis set using Gaussian 09 software package.[30] The rotational energy barrier was studied computationally at the M06/Def2-TZVPP level for BODIPYs **1b-6b**. The main electronic transitions in **1b-6b** are given in the Tables S5 and S6. Figure 5 shows the representative molecular orbital diagram indicating intermolecular charge transfer in the ground state and rotational transition state of **3b**.

The HOMO and LUMO of **1b** are mainly localized on the BODIPY core, whereas HOMO-1 and LUMO+1 are localized mainly on the phenyl ring. The TDDFT calculations reveal that the HOMO-1 to LUMO transition has considerable oscillator strength (f = 0.2320), and the corresponding transition can be considered as intramolecular charge transfer (ICT) from phenyl ring to BODIPY core. However, the rotational barrier for rotation of the phenyl group with respect to the boradiacene unit computed for **1b** is only 1.63 kcal/mol. Hence, the phenyl group undergoes free rotation in a non-viscous solvent. The oscillator strength corresponding to a similar transition in the transition state where the boradiacene unit is perpendicular to the phenyl ring is only 0.0026. All other transitions in the ground and transition state have similar oscillator strength. Hence, the HOMO-1 to LUMO transition is responsible for the variation in fluorescence intensity when the viscosity of solvent changes. In viscous solvents, due to the hindered rotation, the probability of HOMO-1 to LUMO transition will be high (Table S5).

ACCEPTED MANUSCRIPT

J. Porphyrins Phthalocyanines Downloaded from www.worldscientific.com
by UNIVERSITY OF NEW ENGLAND on 04/25/20. Re-use and distribution is strictly not permitted, except for Open Access articles.

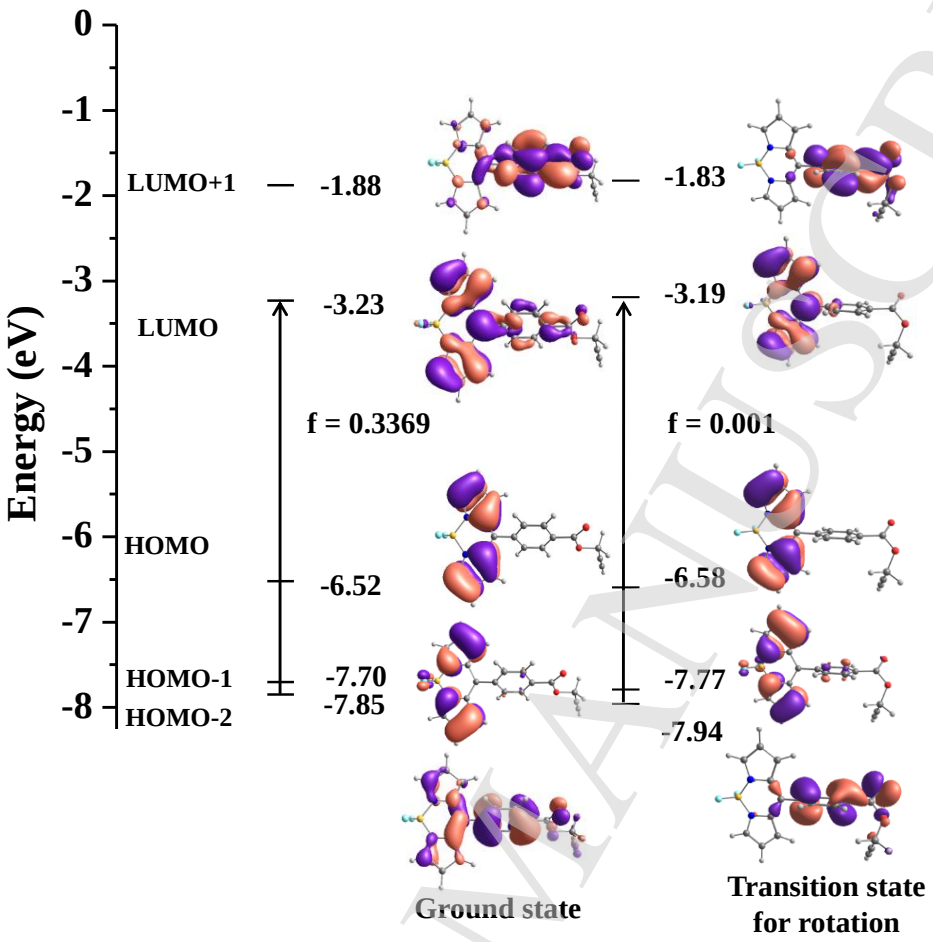

Fig. 5. Molecular orbital diagram of **3b** in the ground state and rotational transition state.

The rotational barriers calculated for 2b-6b are also marginal (0.99 (**2b**), 0.94 (**3b**), 0.94 (**4b**), 0.92 (**5b**) and 1.28 (**6b**)). Hence, similar to **1b**, the compounds **2b-6b** also undergoes rotation of phenyl ring with respect to boradiacene unit. For rotors **3b-6b**, the HOMO-2→LUMO transition accounts for the ICT. The oscillator strength for this transition has significant value, which reduces significantly in the transition state (0.3369 to 0.001 (**3b**), 0.2121 to 0.0007 (**4b**), 0.3038 to 0.0005 (**5b**) and 0.2350 to 0.0006 (**6b**)). On the other hand, ICT from phenyl ring to boradiacene unit arises from HOMO-3→LUMO, in **2b** (f = 0.2032). The theoretical studies indicate that the electronic transition responsible for the enhanced fluorescence intensity of **1b-6b** in the high viscous solvent is attributed to intramolecular charge transfer.

ACCEPTED MANUSCRIPT

J. Porphyrins Phthalocyanines Downloaded from www.worldscientific.com
by UNIVERSITY OF NEW ENGLAND on 04/25/20. Re-use and distribution is strictly not permitted, except for Open Access articles.

Enumeration of bacterial cells using molecular rotors

The practical applicability of the FMRs (**1b-6b**) in microbiology has been illustrated using **3b** and model organism *E. coli*, and we anticipate that this can be extended to clinical analyses.[29] The bacterial strain, *E. coli* was grown in nutrient broth at 37 ºC for 18-24 hours. The cell densities of five serially diluted cultures were estimated using absorbance and McFarland standard table and recorded in CFU/mL. Each sample was treated with **3b** for 30 min, and the unbound probe compound was removed from the biomass by repeated washing and centrifugation with PBS 1X. Fluorescence spectra of the cell suspensions were recorded, and the experiments were performed in triplicate. The fluorescent intensity was compared with cell density and found that an increase in the fluorescent intensity is proportional to the cell density (Figure 6; $R^2 = 0.99$).

One of the common features of BODIPYs is that it will be internalized easily into the bacterial cell.[14] The viscosity of bacterial culture is directly dependent on increasing cell density. From Figure 6, it is obvious that the fluorescence intensity of this compound can be taken as an index of the number of cells per ml. However, the cell density varies with the type of organism in McFarland standards. Therefore, a different calibration curve has to be plotted for determining the cell number for various microbes, and these investigations are underway in our laboratory. The rate of internalization of the probe, as well as the viscosity of the bacterial suspension, can ensure the accuracy of the experiment. Thus, fluorescence measurement allows a quick assessment of microbial growth, enabling bacterial enumeration independent of growth characteristics.

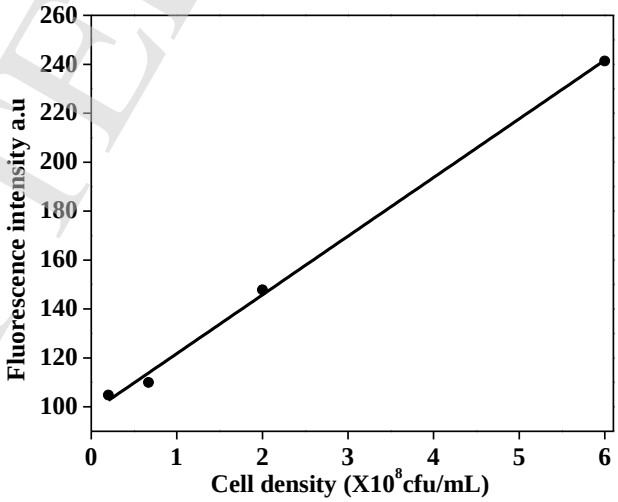

Fig. 6. Fluorescence intensity of **3b** (2.4×10^{-5} M) at different cell density, $\lambda_{ex} = 480$ nm.

ACCEPTED MANUSCRIPT

J. Porphyrins Phthalocyanines Downloaded from www.worldscientific.com
by UNIVERSITY OF NEW ENGLAND on 04/25/20. Re-use and distribution is strictly not permitted, except for Open Access articles.

Conclusions

Herein, we propose meso- 3/4-phenyl substituted BODIPYs (**1b-6b**) as fluorescent molecular rotors to identify viscosity variations. The rotors are insensitive to solvent polarity; hence, they are perfect rotors showing sensitivity comparable to benchmark FMRs. We have also demonstrated the application of rotor **3b** in the bacterial enumeration with *E. coli* as a model organism. The present rotors can also be used to determine local viscosity variations via fluorescence lifetime imaging microscopy (FLIM). The FLIM using rotors **1b-6b** can be further employed in determining the colony-forming unit (CFU) of various microbes. The DFT calculations indicate that the hindered rotation of the phenyl ring with respect to boradiacene unit enhances the intramolecular charge transfer, which in turn leads to high fluorescence intensity in the viscous solvent.

Conflicts of interest

There are no conflicts to declare.

Acknowledgments

Department of Science and Technology (DST), New Delhi through the EMR/2016/002396 project, is gratefully acknowledged for funding to CA. We thank Dr. Babu Varghese, SAIF, IIT Madras for the single crystal data collection, structure solution, and refinement.

References

1. Dziuba D, Jurkiewicz P, Cebecauer M, Hof M and Hocek M. *Angew. Chemie Int. Ed.* 2016; **55**: 174-178.
2. Ferri G, Nucara L, Biver T, Battisti A, Signore G and Bizzarri R. *Biophys. Chem.* 2016; **208**: 17-25.
3. Yang Z, He Y, Lee JH, Chae W-S, Ren W X, Lee J H, Kang C and Kim J S. *Chem. Commun.* 2014; **50**: 11672-11675.
4. Yang Z, He Y, Lee J H, Park N, Suh M, Chae W S, Cao J, Peng X, Jung H, Kang C and Kim JS. *J. Am. Chem. Soc.* 2013; **135**: 9181-9185.
5. Gupta N, Reja S I, Bhalla V, Gupta M, Kaur G and Kumar M. *J. Mater. Chem. B* 2016; **4**: 1968-1977.
6. Kuimova MK, Botchway S W, Parker AW, Balaz M, Collins H A, Anderson H L, Suhling K

ACCEPTED MANUSCRIPT

J. Porphyrins Phthalocyanines Downloaded from www.worldscientific.com
by UNIVERSITY OF NEW ENGLAND on 04/25/20. Re-use and distribution is strictly not permitted, except for Open Access articles.

and Ogilby PR. *Nat. Chem.* 2009; **1**: 69-73.

7. Zhu H, Fan J, Li M, Cao J, Wang J and Peng X. *Chem. A Eur. J.* 2014; **20**: 4691-4696.
8. Mika J T, Thompson A J, Dent M R, Brooks N J, Michiels J, Hofkens J and Kuimova M K. *Biophys. J.* 2016; **111**: 1528-1540.
9. Suhling K. *Biophys. J.* 2016; **111**: 1337-1338.
10. S. Clais, G. Boulet, M. Van kerckhoven, E. Lanckacker, P. Delputte, L. Maes and P. Cos, *Lett. Appl. Microbiol.*2015; 60, 79-84.
11. Lee S C, Heo J, Woo HC, Lee J A, Seo YH, Lee C L, Kim S and Kwon O P. *Chem. A Eur. J.* 2018; **24**: 13706-13718.
12. Bahaidarah E, Harriman A, Stachelek P, Rihn S, Heyer E and Ziessel R. *Photochem. Photobiol. Sci.* 2014; **13**: 1397-1401.
13. Lee C H and S. Lindsey J. *Tetrahedron* 1994; **50**: 11427-11440.
14. Prasannan D, Raghav D, Sujatha S, Hareendrakrishna kumar H, Rathinasamy K and Arunkumar C. *RSC Adv.* 2016; **6**: 80808-80824.
15. Chen Y, Zhao J, Guo H and Xie L. *J. Org. Chem.* 2012; **77**: 2192-2206.
16. Kee H L, Kirmaier C, Yu L, Thamyongkit P, Youngblood W J, Calder ME, Ramos L, Noll B C, Bocian D F, Scheidt WR, Birge R R, Lindsey J S and Holten D. *J. Phys. Chem. B* 2005; **109**: 20433-20443.
17. Zhou F, Shao J, Yang Y, Zhao J, Guo H, Li X, Ji S and Zhang Z. *European J. Org. Chem.* 2011: 4773-4787.
18. Qin W, Baruah M, Van Der Auweraer M, De Schryver F C and Boens N. *J. Phys. Chem. A* 2005; **109**: 7371-7384.
19. Lee S C, Heo J, Ryu J W, Lee C L, Kim S, Tae J-S, Rhee B O, Kim S W and Kwon O P. *Chem. Commun.* 2016; **52**: 13695-13698.
20. Raut S, Kimball J, Fudala R, Doan H, Maliwal B, Sabnis N, Lacko A, Gryczynski I, Dzyuba S V. and Gryczynski Z. *Phys. Chem. Chem. Phys.* 2014; **16**: 27037-27042.
21. Haidekker M A and Theodorakis E A. *Org. Biomol. Chem.* 2007; **5**: 1669-1678.
22. Alkindi A S, Al-Wahaibi Y M and Muggeridge A H. *J. Chem. Eng. Data* 2008; **53**: 2793-2796.
23. Stöckl M T, Bizzarri R and Subramaniam V. In Springer Series on Fluorescence. , 2012; 215-240.
24. Becke A D. *Phys. Rev. A* 1988; **38**: 3098-3100.

ACCEPTED MANUSCRIPT

25. Perdew J P. *Phys. Rev. B* 1986; **33**: 8822-8824.
26. Schäfer A, Horn H and Ahlrichs R. *J. Chem. Phys.* 1992; **97**: 2571-2577.
27. Zhao Y and Truhlar D G. *Theor. Chem. Acc.* 2008; **120**: 215-241.
28. Weigend F, Häser M, Patzelt H and Ahlrichs R. *Chem. Phys. Lett.* 1998; **294**: 143-152.
29. Bodio E, Denat F and Goze C. *J. Porphyr. Phthalocyanines* 2019; **23**: 1159-1183.
30. Frisch M J, Trucks G W, Schlegel H B, Scuseria G E, Robb M A, Cheeseman J R, Scalmani G, Barone V, Mennucci B, Petersson G A, Nakatsuji H, Caricato M, Li X, Hratchian H P, Izmaylov A F, Bloino J, Zheng G, Sonnenberg J L, Hada M, Ehara M, Toyota K, Fukuda R, Hasegawa J, Ishida M, Nakajima T, Honda Y, Kitao O, Nakai H, Vreven T, Montgomery J A, Jr., Peralta J E, Ogliaro F, Bearpark M, Heyd J J, Brothers E, Kudin K N, Staroverov V N, Keith T, Kobayashi R, Normand J, Raghavachari K, Rendell A, Burant J C, Iyengar S S, Tomasi J, Cossi M, Rega N, Millam J M, Klene M, Knox J E, Cross J B, Bakken V, Adamo C, Jaramillo, J, Gomperts R, Stratmann R E, Yazyev O, Austin A J, Cammi R, Pomelli C, Ochterski J W,. Martin R L, Morokuma K, Zakrzewski V G, Voth G A, Salvador P, Dannenberg J J, Dapprich S, Daniels A D, Farkas O, Foresman J B, Ortiz J V, Cioslowski J and Fox, D J Gaussian 09 (Revision B.01), Gaussian, Inc., Wallingford CT, 2010.

J. Porphyrins Phthalocyanines Downloaded from www.worldscientific.com
by UNIVERSITY OF NEW ENGLAND on 04/25/20. Re-use and distribution is strictly not permitted, except for Open Access articles.

ACCEPTED MANUSCRIPT

Accepted manuscript to appear in JPP

J. Porphyrins Phthalocyanines Downloaded from www.worldscientific.com
by UNIVERSITY OF NEW ENGLAND on 04/25/20. Re-use and distribution is strictly not permitted, except for Open Access articles.

Electronic Supplementary Information

For

Development of alkyne-BODIPYs as viscosity sensitive fluorescent probes for enumeration of bacterial cells

Dijo Prasannan,[a] Suchithra Tharamel Vasu,[b] Chellaiah Arunkumar[a] and Pattiyil Parameswaran[c]*

[a]*Bioinorganic Materials Research Laboratory, Department of Chemistry, National Institute of Technology Calicut, NIT Campus P.O., Calicut, India-673 601.*
[b]*School of Biotechnology, National Institute of Technology Calicut, NIT Campus P.O., Calicut, India-673 601.*
[c]*Theoretical and Computational Chemistry Laboratory, Department of Chemistry, National Institute of Technology Calicut, NIT Campus P.O., Calicut, India-673 601.*

Contents

EXPERIMENTAL

Materials and Methods

Pyrrole purchased from Spectrochem (India) was distilled over CaH_2 before use. 4-Hydroxybenzaldehyde, 3-Hydroxybenzaldehyde, Propargyl bromide and 3-Dichloro-5,6-dicyano-1,4-benzoquinone (DDQ) were obtained from Sigma Aldrich and were used as such. 3-Carboxaldehyde procured from Alfa Aesar was used without further purification. Trifluroacetic acid (TFA) was purchased from AVRA Synthesis Pvt. Ltd. and was distilled over P_2O_5. Triethylamine (Et_3N) purchased from Qualigens was used without further purification. 4-Formyl benzoicacid and Boron trifluoride etherate ($BF_3.OEt_2$) were purchased from Spectrochem (India). $BF_3.OEt_2$ and dimethylformamide (DMF) (SRL, India) were purified by vacuum distillation over CaH_2 whereas 4-Formyl benzoicacid was used as such. Chloroform, dichloromethane, hexane, and ethanol were purchased from Merck (India) and purified by distilling over K_2CO_3 (except ethanol). THF was obtained from and was used as such.

^{1}H NMR spectra were recorded with a Bruker 400 MHz FT-NMR spectrometer in $CDCl_3$ / CD_3COCD_3 using tetramethylsilane as the internal reference. IR data was collected on a JASCO FT/IR-4700 with KBr pellets. UV-Visible spectra were recorded on a Shimadzu double beam spectrometer 2450 instrument using 1 cm matched quartz cuvettes at room temperature. Fluorescence spectra were recorded on a Perkin-Elmer LS-55 Luminescence spectrophotometer

ACCEPTED MANUSCRIPT

J. Porphyrins Phthalocyanines Downloaded from www.worldscientific.com
by UNIVERSITY OF NEW ENGLAND on 04/25/20. Re-use and distribution is strictly not permitted, except for Open Access articles.

with a slit width of 10 at 470 nm excitation wavelength and emission from 490 to 750 nm. The fluorescence quantum yield (Φ_f) was computed using the below equation,

$$\Phi_f = \Phi_f^R F_S A_R \eta_S^2 / F_R A_S \eta_R^2$$

where F_S and F_R are the integrated fluorescence intensities of the sample and reference, A_S and A_R are the absorbance of the sample and reference at excitation wavelength, η_S and η_R are the refractive indexes of the solvents used for the sample and reference. Fluorescein in 0.1 M NaOH solution was used as the reference (Φ_f = 0.85, λ_{exc}= 470 nm). All Φ_f values were corrected for changes in refractive index. Both the BODIPYs and reference solutions were prepared with the same absorbance at the excitation wavelength (between 0.1 and 0.05 in a 1 cm quartz cell). The fluorescence lifetime was done on a MicroTime 200 timeresolved confocal fluorescence setup from PicoQuant equipped with an inverted microscope from Olympus IX 71 containing a water immersion objective of Olympus UplansApo NA 1.2 60X. A 485 nm pulsed diode laser (PicoQuant) was used as the excitation source with a stable 10 MHz repetition rate and 60 nW excitation power.

Electrochemical measurements were performed on a CH-instruments Inc, USA (Model: CHI660E) equipped with potentiostat / galvanostat with Fourier Transform AC Voltammeter. The electrochemical system utilized a three-electrode configuration consisting of a glassy carbon (working), platinum wire (auxillary) and standard Calomel reference (SCE) electrodes. The concentrations of the samples were maintained as 0.1 M containing tetrabutylammonium hexafluorophosphate (NBu_4PF_6) as supporting electrolyte (0.1 M) in dichloromethane at 25 °C under N_2 atmosphere at a scan rate of 50 mV/s. The crystal structure data was collected on a Bruker AXS Kappa Apex II CCD diffractometer with Mo K_α radiation (λ = 0.7107 Å). The structures were solved using direct methods and refined by full matrix least-squares using the program SHELXL-97/SIR 92 (WINGX). The fluorescence imaging was performed using an Olympus- IX73 microscope attached with a digital camera at 100x magnification. The images were processed using cellSens software.

General procedure for the synthesis of substituted benzaldehydes

The substituted aldehydes were synthesized using the standard procedure[1] described below. To the corresponding benzaldehyde (1 equiv.) in DMF was added potassium carbonate (0.5 equivalents). To this stirring solution under nitrogen, propargyl bromide (1.1 equivalents) was

ACCEPTED MANUSCRIPT

J. Porphyrins Phthalocyanines Downloaded from www.worldscientific.com
by UNIVERSITY OF NEW ENGLAND on 04/25/20. Re-use and distribution is strictly not permitted, except for Open Access articles.

added and refluxed at 80ºC for 3 – 6 h. The reaction mixture after cooling to room temperature was diluted with water, extracted with CH_2Cl_2 and the combined organic layers were washed several times with water to remove DMF. The organic phase was then dried over Na_2SO_4, solvent was evaporated and the residue was purified by silica gel column chromatography using chloroform/hexane as eluent to obtain the pure compound.

Compound 1, 2: The crude residue was purified by silica gel column chromatography using chloroform/hexane, 60/40 as eluent to obtain the pure compounds **1** and **2** in 77 % yield.

Compound 3, 4: The reaction mixture was refluxed for 6 h and the crude compounds after standard work up were purified on silica gel chromatography using 66/34 chloroform/hexane as eluent. Yield = 83 % for compound **3** and 70 % for compound **4**.

General procedure for the synthesis of dipyrromethanes, 1a - 6a

To a solution of corresponding benzaldehyde (1 equivalent) in pyrrole (25/50 equivalent) under N_2 atmosphere, was added catalytic amount of trifluoroacetic acid (TFA, 0.1 equivalents). The mixture was stirred at room temperature for 10-15 minutes. Upon completion of the reaction, dilute NaOH (0.1 M) was added to quench the reaction. The product was extracted with ethyl acetate washed with water, dried over Na_2SO_4, and evaporated to dryness under vacuum. To this crude product 2-3 drops of triethylamine was added to arrest the degradation of dipyrromethane. The compound was purified by column chromatography on silica gel using $CHCl_3$/hexane. For dipyrromethanes, 5a and 6a, the concentrated pale brown oil was dissolved in a 1:20 mixture of water and ethanol and was allowed to crystallize at 0 °C overnight, affording solid that was filtered and dried in vacuo.

General procedure for the synthesis of BODIPYs, 1b - 6b

The BODIPYs were prepared by following the standard procedure.[2] Briefly, to the corresponding dipyrromethane dissolved in DCM, nitrogen was purged for 15 min. 3-Dichloro-5,6-dicyano-1,4-benzoquinone (DDQ), (1.1 equivalents) was then added and stirred vigorously for 30 min at room temperature. To this oxidized product, triethylamine was added. After 15 min, boron trifluroetherate was added and stirring was continued. The observation of orange red fluorescent spot confirms the formation of desired BODIPY. The reaction mixture was extracted with dichloromethane, the combined organic fractions were then washed with water, dried over

ACCEPTED MANUSCRIPT

J. Porphyrins Phthalocyanines Downloaded from www.worldscientific.com
by UNIVERSITY OF NEW ENGLAND on 04/25/20. Re-use and distribution is strictly not permitted, except for Open Access articles.

Na_2SO_4, filtered and the solvent was removed under reduced pressure to give the crude product. This was further purified by silica gel column chromatography using chloroform (unless specified) to afford pure compound as orange red fluorescent solid.

***meso*-(4-Propargyloxyphenyl)dipyrromethane, 1a:** The compound was purified by with 70/30 chloroform/hexane to yield pale yellow coloured compound **1a**. Yield = 34 %. ^{1}H-NMR (400 MHz, $CDCl_3$, δ in ppm) 7.87 (br s, 2H; NH protons), 7.13-6.66 (d, 4H; Ar-H), 6.66 (br d, 2H; CH α to pyrrole NH), 6.15 (br m, 2H; CH β to pyrrole NH), 5.88 (s, 2H; py-H), 5.39 (s, 1H; meso-H), 4.65 (d, J = 2.4 Hz, 2H), 2.5 (t, J = 2.0 Hz 2.4 Hz, 1H, long range coupling).

***meso*-(3-Propargyloxyphenyl)dipyrromethane, 2a:** The crude compound was purified by silica gel column chromatography using chloroform. Yield = 68.56 %. ^{1}H-NMR (400 MHz, $CDCl_3$, δ in ppm) 7.92 (br s, 2H; NH protons), 7.26-6.84 (br m, 4H; Ar-H), 6.68 (br d, 2H; CH α to pyrrole NH), 6.15 (br m, 2H; CH β to pyrrole NH), 5.93 (s, 2H; py-H), 5.44 (s, 1H; meso-H), 4.63 (d, J = 2.4 Hz, 2H), 2.48 (t, J = 2.4 Hz, 1H).

***meso*-(Prop-2-yn-1-yl-4-formylbenzoate)dipyrromethane, 3a:** The crude residue was chromatographed using 58:48 chloroform: hexane as eluent to obtain the pure compound **3a**. Yield = 51 % . ^{1}H-NMR (400 MHz, $CDCl_3$, δ in ppm) 7.25 (br, d, 2H; NH protons), 7.9 (d, 2H; Ar-H, NH protons), 6.68 (br d, 2H; CH α to pyrrole NH), 6.13 (br m, 2H; CH β to pyrrole NH), 5.86 (s, 2H; py-H), 5.49 (s, 1H; meso-H), 4.87 (d, 2H), 2.48 (t, 1H).

***meso*-(Prop-2-yn-1-yl-3-formylbenzoate)dipyrromethane, 4a:** The pale yellow oily dipyrromethane was eluted with 60/40 chloroform/hexane to yield the pure compound **4a**. Yield = 72 % (0.5133 g). ^{1}H-NMR (400 MHz, $CDCl_3$, δ in ppm) 8.10 (br, s, 2H; NH protons), 7.99 (s, 1H; Ar-H), 7.91(d, 1H; Ar-H), 7.32 (m, 2H; Ar-H) 6.63 (d, 2H; CH α to pyrrole NH), 6.11 (m, 2H; CH β to pyrrole NH), 5.83 (s, 2H; py-H), 5.43 (s, 1H; meso-H), 4.82 (d, 2H), 2.46 (t, 1H).

5-(4-Carboxyphenyl)dipyrromethane, 5a: Yield = 50 %. ^{1}H NMR (acetone-d_6) δ (ppm): 5.549 (s, 1H), 5.751(s, 2H), 5.981 (t, 2H), 6.697 (s, 2H), 7.321 (d, 2H), 7.938 (d, 2H), 9.77 (s, br, 2H).

***meso*-(4-Propargyloxyphenyl) BODIPY, 1b:**. Yield = 34.49 % ^{1}H-NMR (400 MHz, $CDCl_3$, δ in ppm) 2.596 (1H, t), 4.803 (2H, d), 6.559 (2H, d; py-H), 6.981 (2H, d; py-H), 7.930 (1H, s; py-H), 7.149 (2H, d; Ar-H), 7.576 (2H, d; Ar-H); 55.91, 76.30, 76.94, 114.80, 118.28, 127.12, 131.19,

ACCEPTED MANUSCRIPT

J. Porphyrins Phthalocyanines Downloaded from www.worldscientific.com
by UNIVERSITY OF NEW ENGLAND on 04/25/20. Re-use and distribution is strictly not permitted, except for Open Access articles.

132.19, 134.85, 143.62, 147.12, 160.03. TOF-MS (ES): m/z : Calcd= 322.12; found: 322.00. IR (KBr): 3448, 3276, 3130, 2120, 1601, 1577, 1544, 1475, 1449, 1413, 1390, 1353, 1298, 1261, 1225, 1178, 1079, 976, 840, 762, 744, 709, 678, 593, 535, 429.

***meso*-(3-Propargyloxyphenyl) BODIPY, 2b:** The crude product after standard work up was purified by silica gel column chromatography (chloroform: hexane = 7:3) to yield the pure orange red fluorescent dye. Yield = 15 % (42.83 mg). ^{1}H-NMR (400 MHz, $CDCl_3$, δ in ppm) 2.572 (1H, t), 4.761(2H, d), 6.545 (2H, d; py-H), 6.997 (2H, d; py-H), 7.947 (2H, s; py-H) 7.198 - 7.438 (4H, m; Ar-H). ^{13}C-NMR (400 MHz, $CDCl_3$, δ in ppm) 55.94, 76.29, 78.14, 116.83, 117.54, 118.57, 123.82, 129.56, 131.66, 134.86, 144.29, 146.80, 157.29. TOF-MS (ES): m/z : Calcd= 322.12; found: 322.00. IR (KBr): 3850, 3272, 3105, 2973, 2119, 1601, 1584, 1557, 1475, 1450, 1408, 1387, 1354, 1290, 1263, 1229, 1169, 1081, 990, 849, 773, 751, 670, 612, 593, 533, 416.

***meso*-(Prop-2-yn-1-yl-4-formylbenzoate)BODIPY, 3b:** Yield = 14.5 %. ^{1}H-NMR (400 MHz, $CDCl_3$, δ in ppm) 2.55 (1H, t), 4.99 (2H, d), 6.56 (2H, d; py-H), 6.87 (2H, d; CH β to pyrrole NH), 7.65 (2H, s; CH α to pyrrole NH) 7.97 - 8.22 (2H, m; Ar-H). ^{13}C-NMR (400 MHz, $CDCl_3$, δ in ppm) 52.92, 75.45, 77.50, 76.74, 119.00, 129.83, 130.47, 131.38, 134.59, 138.40, 144.92, 164.95. TOF-MS (ES): m/z : Calcd= 350.10; found: 350.21. IR (KBr): 3432, 3293, 3118, 2947, 2129, 1725, 1573, 1543, 1478, 1439, 1414, 1389, 1353, 1368, 1262, 1227, 1161, 1095, 977, 871, 771, 754, 1725, 642, 591, 420.

***meso*-(Prop-2-yn-1-yl-3-formylbenzoate)BODIPY, 4b**: After completion of the reaction, the crude product was purified by silica gel column chromatography using chloroform/hexane (90/10) to afford orange red solid. Yield = 14 %. ^{1}H-NMR (400 MHz, $CDCl_3$, δ in ppm) 2.53 (1H, t), 4.96 (2H, d), 6.56 (2H, d; py-H), 6.87 (2H, d; CH β to pyrrole NH), 7.97 (2H, s; CH α to pyrrole NH), 7.63 (1H, t; Ar-H), 7.77 (d, 1H; Ar-H), 8.26 (t, 2H; Ar-H). ^{13}C-NMR (400 MHz, $CDCl_3$, δ in ppm) 52.94, 75.45, 76.72, 77.35, 118.95, 128.81, 131.37, 131.45, 134.20, 134.82, 144.81, 145.69, 164.86. TOF-MS (ES): m/z : Calcd= 350.10; found: 350.21. IR (KBr): 3423, 3250, 3105, 2932, 2133, 1720, 1601, 1584, 1556, 1534, 1476, 1409, 1385, 1353, 1161, 1294, 1263, 1221, 986, 853, 781, 750, 599, 429. The crude product was purified by silica gel column chromatography (chloroform : acetone = 90/10) to yield the pure orange fluorescent dye.

ACCEPTED MANUSCRIPT

J. Porphyrins Phthalocyanines Downloaded from www.worldscientific.com
by UNIVERSITY OF NEW ENGLAND on 04/25/20. Re-use and distribution is strictly not permitted, except for Open Access articles.

8-(4-Carboxyphenyl) BODIPY, 5b: Yield = 72 %. ^{1}H NMR in $CDCl_3$ (300 MHz): δ ppm: 8.27 (d, 2H), 7.98 (s, 2H), 7.69 (d, 2H), 6.90 (s, 2H), 6.58 (s, 2H).). ^{13}C-NMR (400 MHz, $CDCl_3$, δ in ppm) 29.36, 30.94, 119.05, 130.19, 131.24, 134.72, 138.80, 144.98, 145.50, 169.96. IR (KBr, cm^{-1}): 3435, 3116, 2928, 2665, 2538, 2371, 2345, 1688, 1573, 1546, 1478, 1412, 1388, 1356, 1284, 1262, 1224, 1158, 1115, 1081, 1046, 1071, 978, 912, 752, 731, 417.

8-(3-Carboxyphenyl) BODIPY, 6b: Yield = 60 %. UV/vis ($CHCl_3$): λ_{max} (log ε) = 505 nm (4.81); Fluorescence ($CHCl_3$): λ_{em}= 522 nm (λ_{ex} = 505 nm)^{1}H NMR in $CDCl_3$ (300 MHz): δ ppm: 8.34 (d, 2H), 7.98 (s, 2H), 7.83 (m 1H), 7.68 (m 1H), 6.89 (d, 2H), 6.58 (d, 2H). ^{13}C-NMR (400 MHz, $CDCl_3$, δ in ppm) 76.70, 118.99, 128.91, 129.78, 131.82, 132.21, 134.23, 135.32, 144.87, 145.68, 170.37. IR (KBr, cm^{-1}): 3433, 3118, 2931, 2738, 2676, 2490, 2370, 2345, 2233, 1700, 1604, 1550, 1451, 1413, 1387, 1357, 1258, 1224, 1111, 1078, 992, 940, 893, 776, 730, 689, 633, 411.

Figure S1. ^{1}H NMR spectrum of **1a**.
Figure S2. ^{1}H NMR spectrum of **2a**.
Figure S3. ^{1}H NMR spectrum of **3a**.
Figure S4. ^{1}H NMR spectrum of **4a**.
Figure S5. ^{1}H NMR spectrum of **5a**.
Figure S6. ^{1}H NMR spectrum of **1b**.
Figure S7. ^{1}H NMR spectrum of **2b**.
Figure S8. ^{1}H NMR spectrum of **3b**.
Figure S9. ^{1}H NMR spectrum of **4b**.
Figure S10. ^{1}H NMR spectrum of **5b**.
Figure S11. ^{1}H NMR spectrum of **6b**.
Figure S12. C-13 NMR spectrum of **1b**.
Figure S13. C-13 NMR spectrum of **2b**.
Figure S13. C-13 NMR spectrum of **3b**.
Figure S14. C-13 NMR spectrum of **4b**.
Figure S15. C-13 NMR spectrum of **5b**.
Figure S16. C-13 NMR spectrum of **6b**.
Figure S17. Mass spectrum of **1b**.
Figure S18. Mass spectrum of **2b**.

ACCEPTED MANUSCRIPT

J. Porphyrins Phthalocyanines Downloaded from www.worldscientific.com
by UNIVERSITY OF NEW ENGLAND on 04/25/20. Re-use and distribution is strictly not permitted, except for Open Access articles.

Figure S19. Mass spectrum of **3b**.

Figure S20. Mass spectrum of **4b**.

Figure S21. Mass spectrum of **5b**.

Figure S22. Mass spectrum of **6b**.

Figure S23. Figure S23. Packing diagrams of (a) **1b**, viewed down 'c' axis; (b) **2b**, viewed along 'a' axis; (c) **3b**, viewed along 'b' axis; (d) **4b**, viewed along 'b' axis; (e) **5b**, viewed down 'a' axis and (f) **6b**, viewed along 'a' axis.

Figure S24. Normalized UV-Visible (solid) and fluorescence (dash) spectra of compounds, **1b-4b**.

Figure S25. (a) Fluorescence intensity *versus* wavelength (b) log (quantum yield) *versus* log (viscosity) for **1b**.

Figure S26. (a) Fluorescence intensity *versus* wavelength (b) log (quantum yield) *versus* log (viscosity) for **2b**.

Figure S27. (a) Fluorescence intensity *versus* wavelength (b) log (quantum yield) *versus* log (viscosity) for **4b**.

Figure S28. (a) Fluorescence intensity *versus* wavelength (b) log (quantum yield) *versus* log (viscosity) for **5b**.

Figure S29. (a) Fluorescence intensity *versus* wavelength (b) log (quantum yield) *versus* log (viscosity) for **6b**.

Figure S30. Log FI *versus* log viscosity of (a) **1b** (b) **2b** (c) **3b** (d) **4b** (e) **5b** (f) **6b**.

Figure S31.

Table S1. Electrochemical redox data of BODIPYs, **1b-6b**.

Table S2. Crystallographic data of compounds, **1b-6b**.

Table S3. Distances (in Å) for different types of interactions in **1b**, **2b**, **3b**, **4b**, **5b** and **6b**.

Table S4. Photophysical properties of **1b-6b** in different solvents.

Table S5. Calculated oscillator strength (f), excitation energy, wavelength, coefficient and its percentage contribution of transitions in transition state.

ACCEPTED MANUSCRIPT

J. Porphyrins Phthalocyanines Downloaded from www.worldscientific.com
by UNIVERSITY OF NEW ENGLAND on 04/25/20. Re-use and distribution is strictly not permitted, except for Open Access articles.

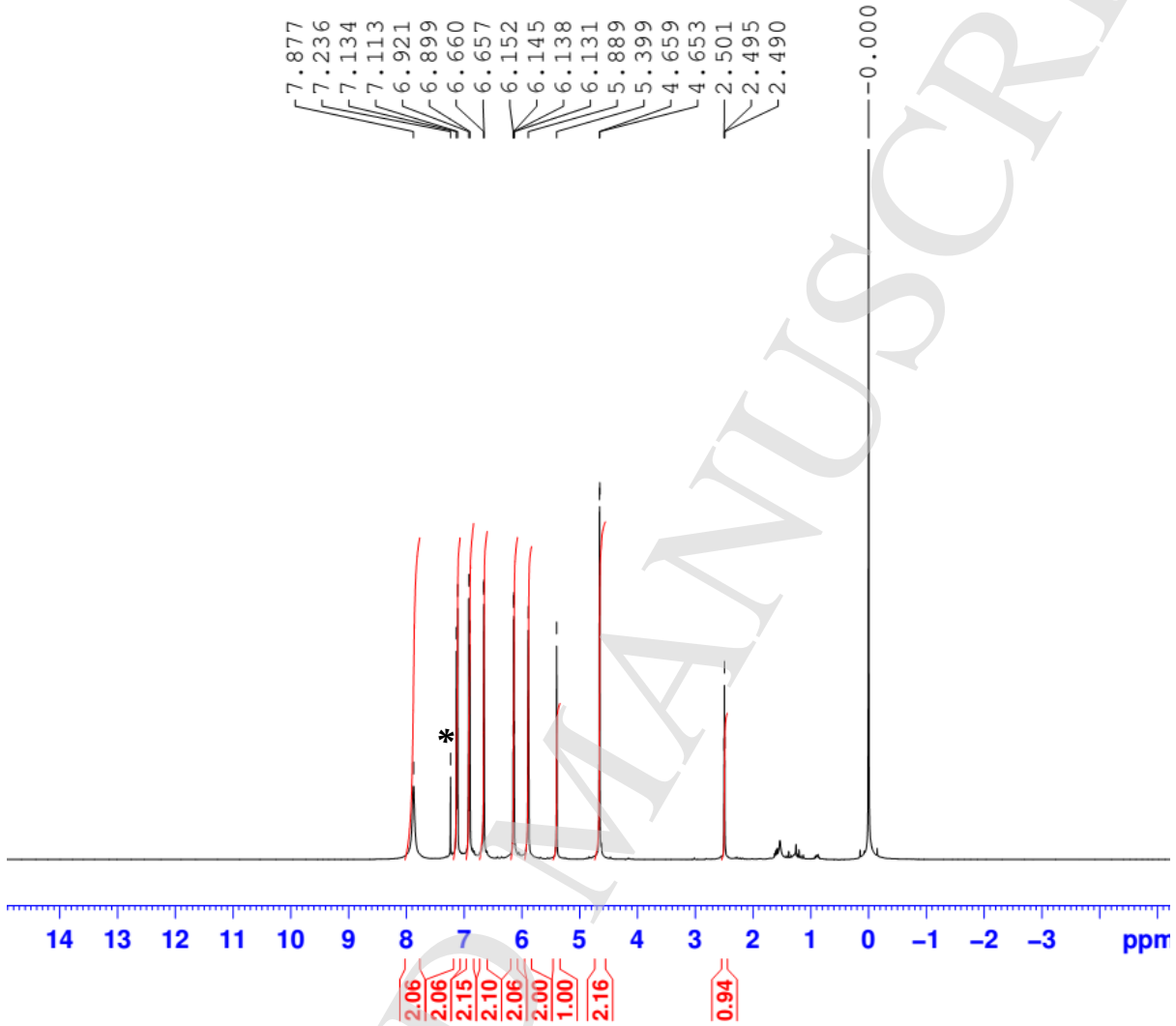

Figure S1 ^{1}H NMR spectrum of compound **1a**

ACCEPTED MANUSCRIPT

J. Porphyrins Phthalocyanines Downloaded from www.worldscientific.com
by UNIVERSITY OF NEW ENGLAND on 04/25/20. Re-use and distribution is strictly not permitted, except for Open Access articles.

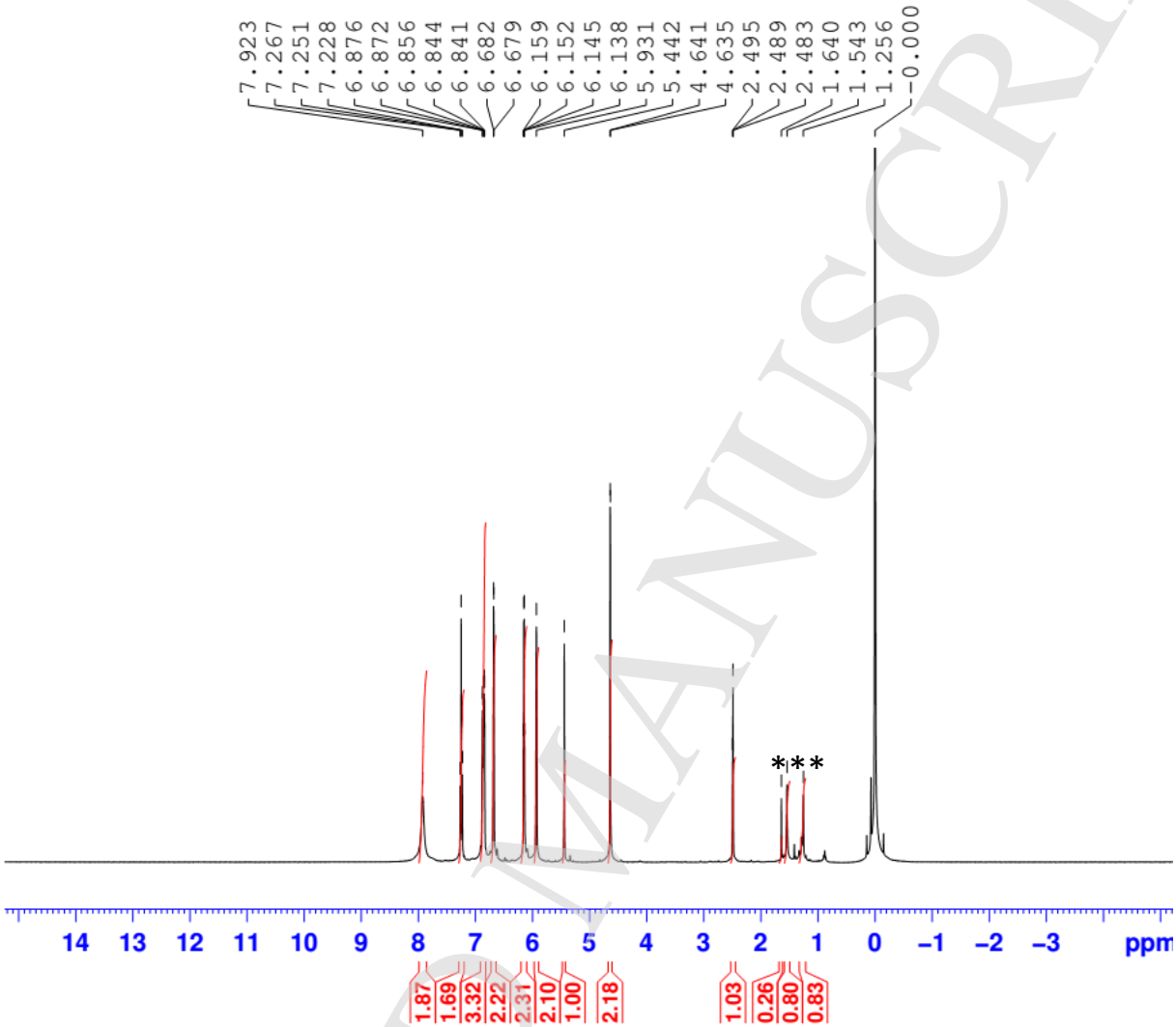

Figure S2 ^{1}H NMR spectrum of compound **2a**

ACCEPTED MANUSCRIPT

J. Porphyrins Phthalocyanines Downloaded from www.worldscientific.com
by UNIVERSITY OF NEW ENGLAND on 04/25/20. Re-use and distribution is strictly not permitted, except for Open Access articles.

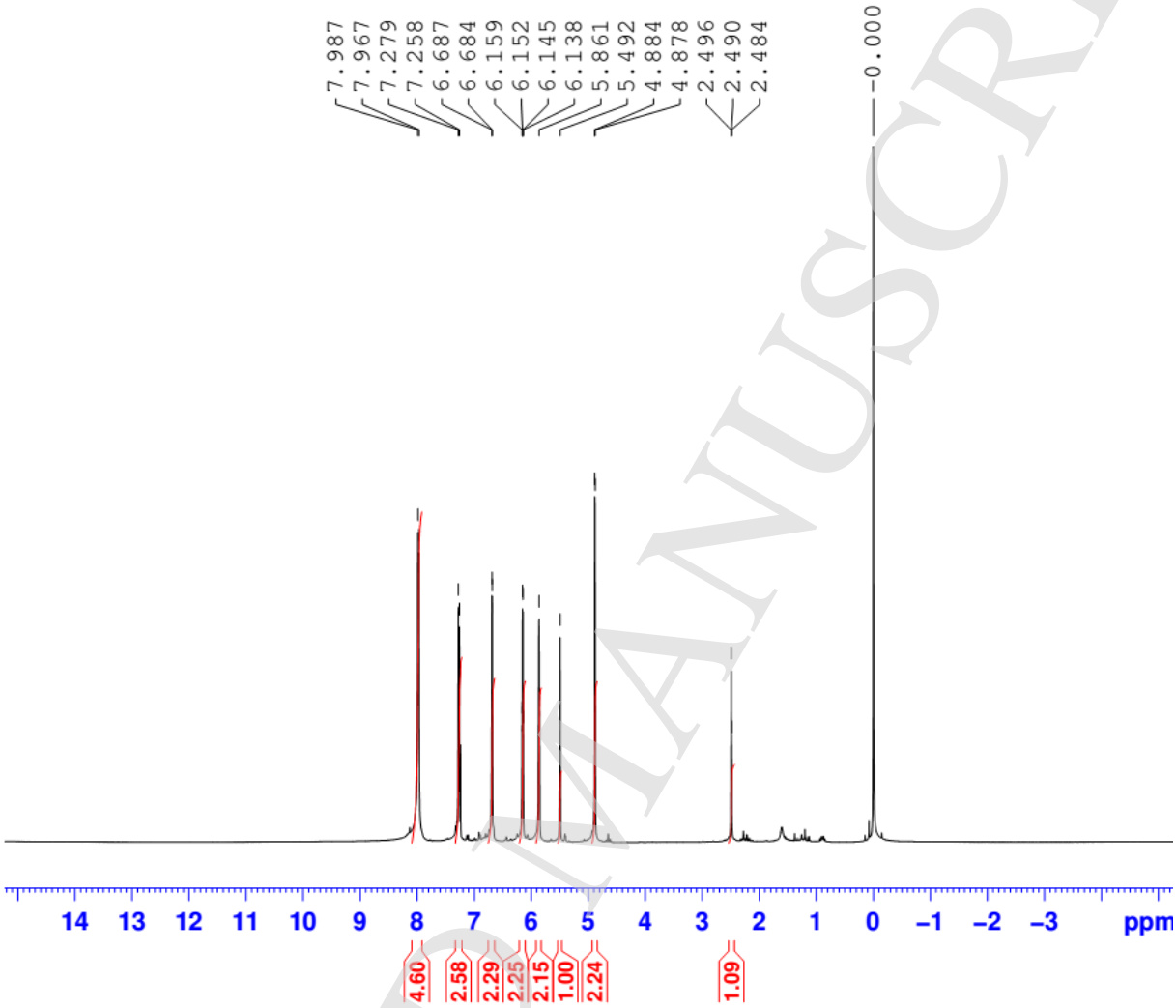

Figure S3 ^{1}H NMR spectrum of compound **3a**

ACCEPTED MANUSCRIPT

J. Porphyrins Phthalocyanines Downloaded from www.worldscientific.com
by UNIVERSITY OF NEW ENGLAND on 04/25/20. Re-use and distribution is strictly not permitted, except for Open Access articles.

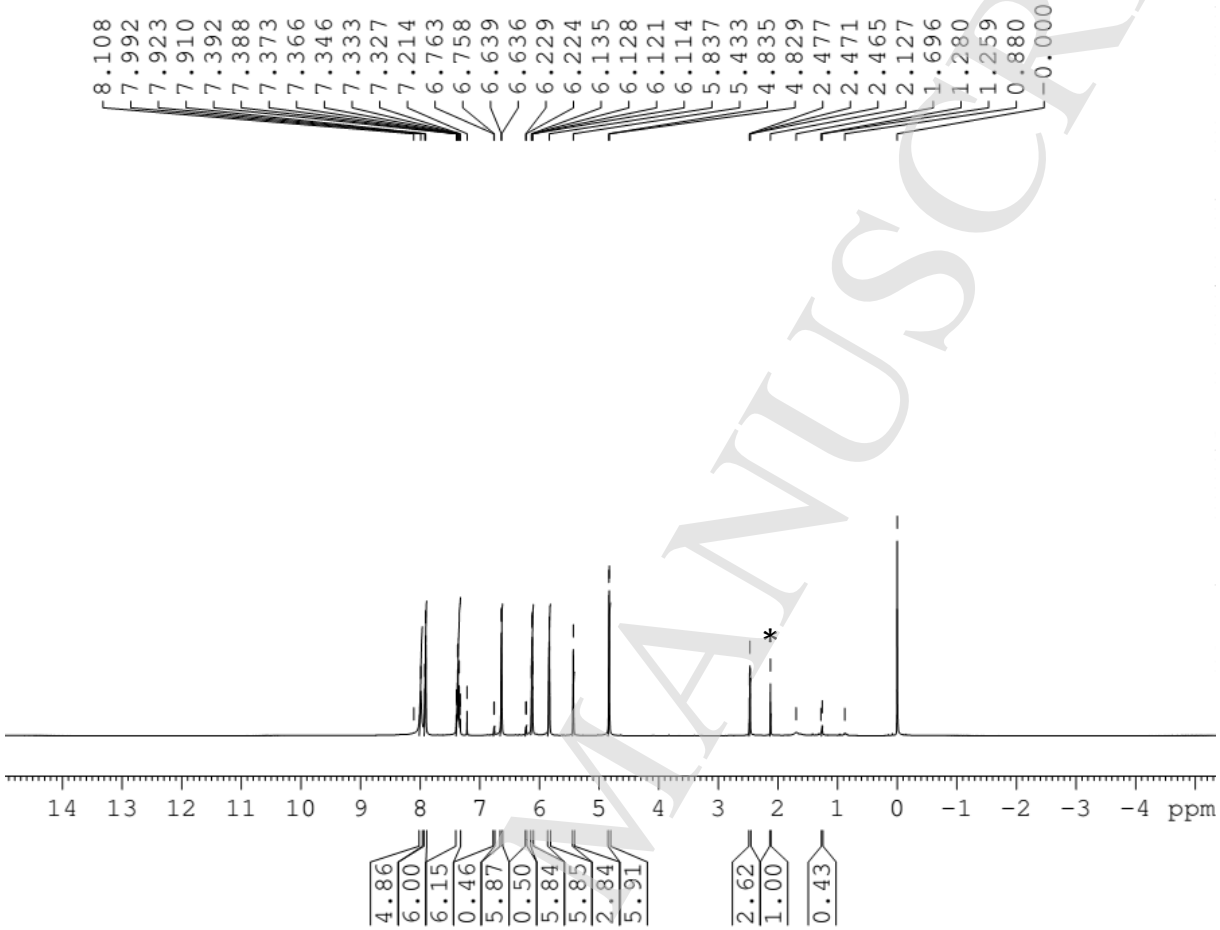

Figure S4 ^{1}H NMR spectrum of compound **4a**

ACCEPTED MANUSCRIPT

J. Porphyrins Phthalocyanines Downloaded from www.worldscientific.com
by UNIVERSITY OF NEW ENGLAND on 04/25/20. Re-use and distribution is strictly not permitted, except for Open Access articles.

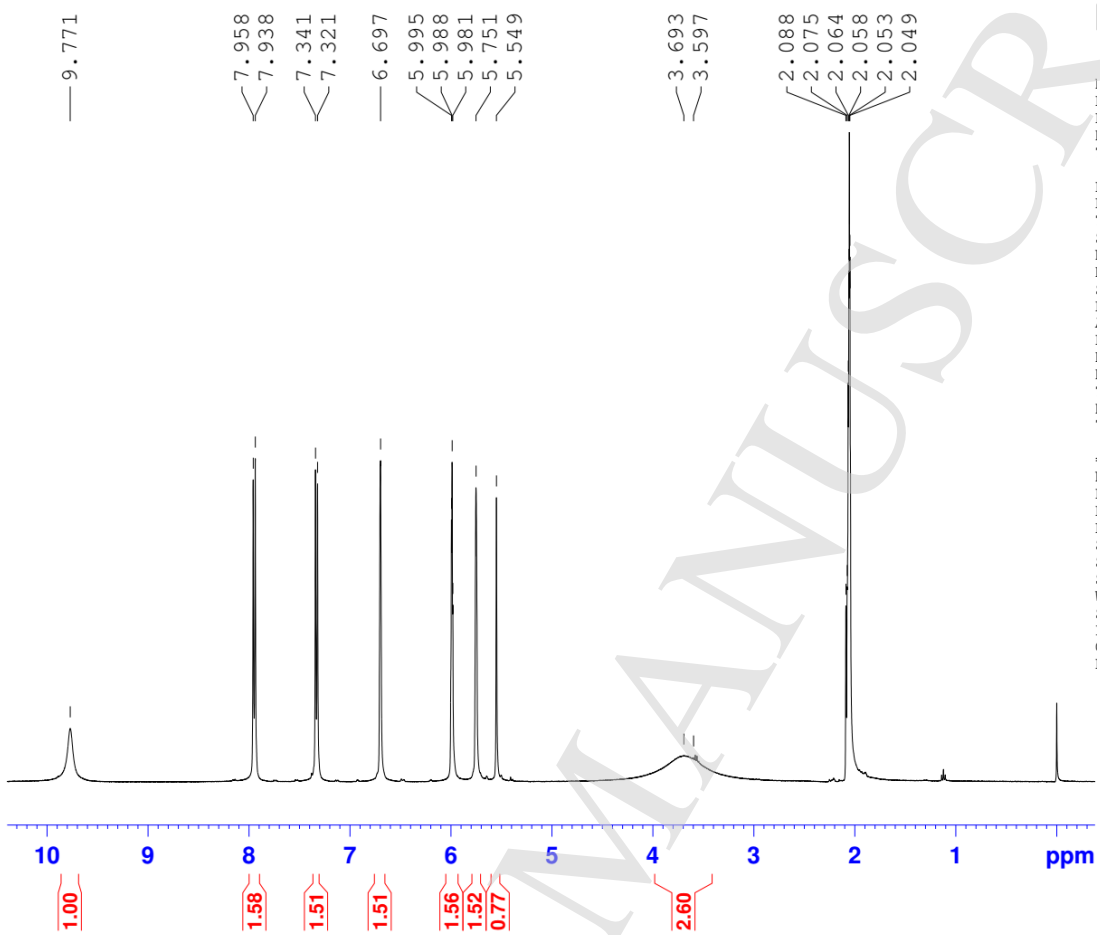

Figure S5 ^{1}H NMR spectrum of compound **5a**

ACCEPTED MANUSCRIPT

J. Porphyrins Phthalocyanines Downloaded from www.worldscientific.com
by UNIVERSITY OF NEW ENGLAND on 04/25/20. Re-use and distribution is strictly not permitted, except for Open Access articles.

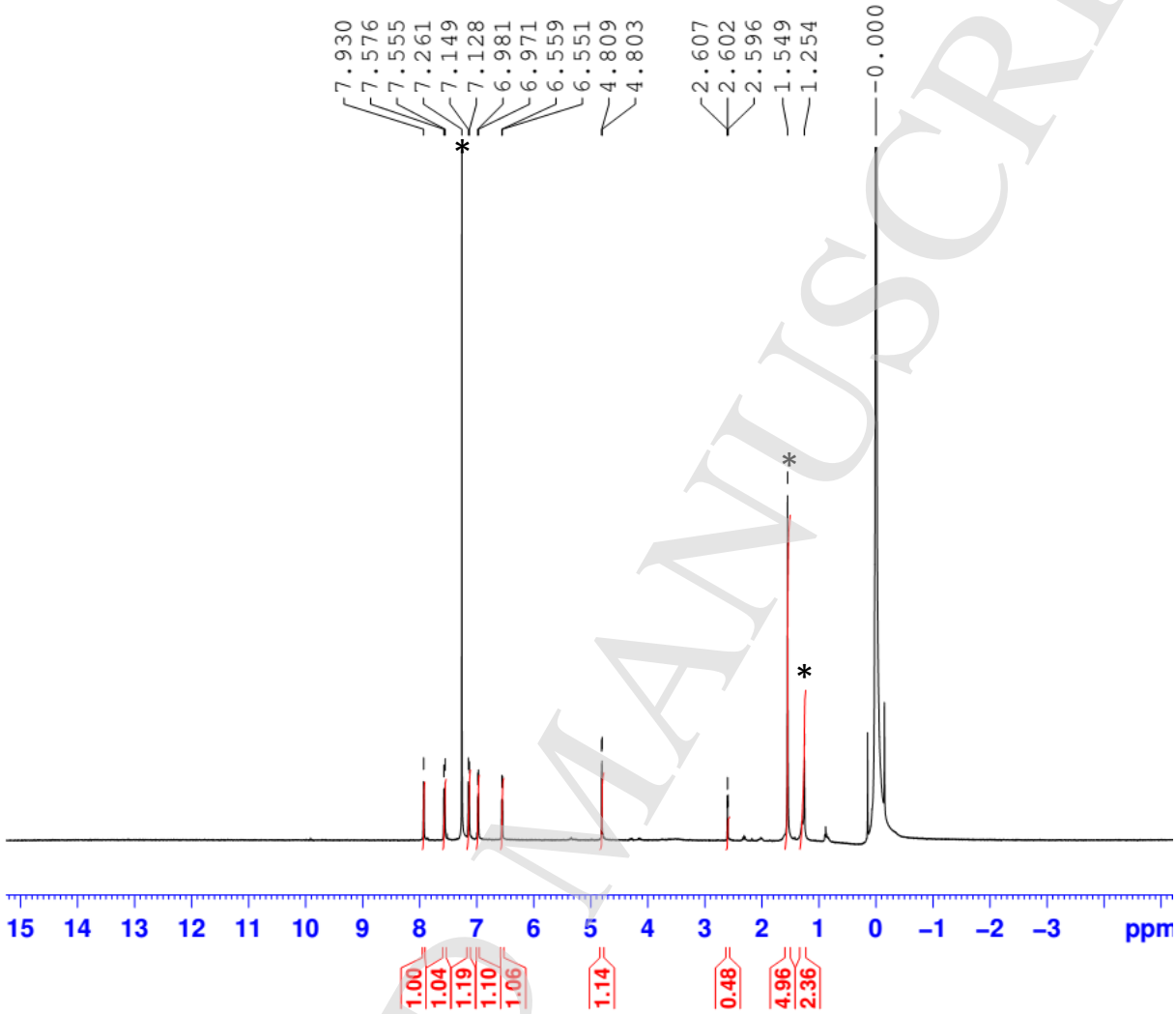

Figure S6 ^{1}H NMR spectrum of compound **1b**

ACCEPTED MANUSCRIPT

J. Porphyrins Phthalocyanines Downloaded from www.worldscientific.com
by UNIVERSITY OF NEW ENGLAND on 04/25/20. Re-use and distribution is strictly not permitted, except for Open Access articles.

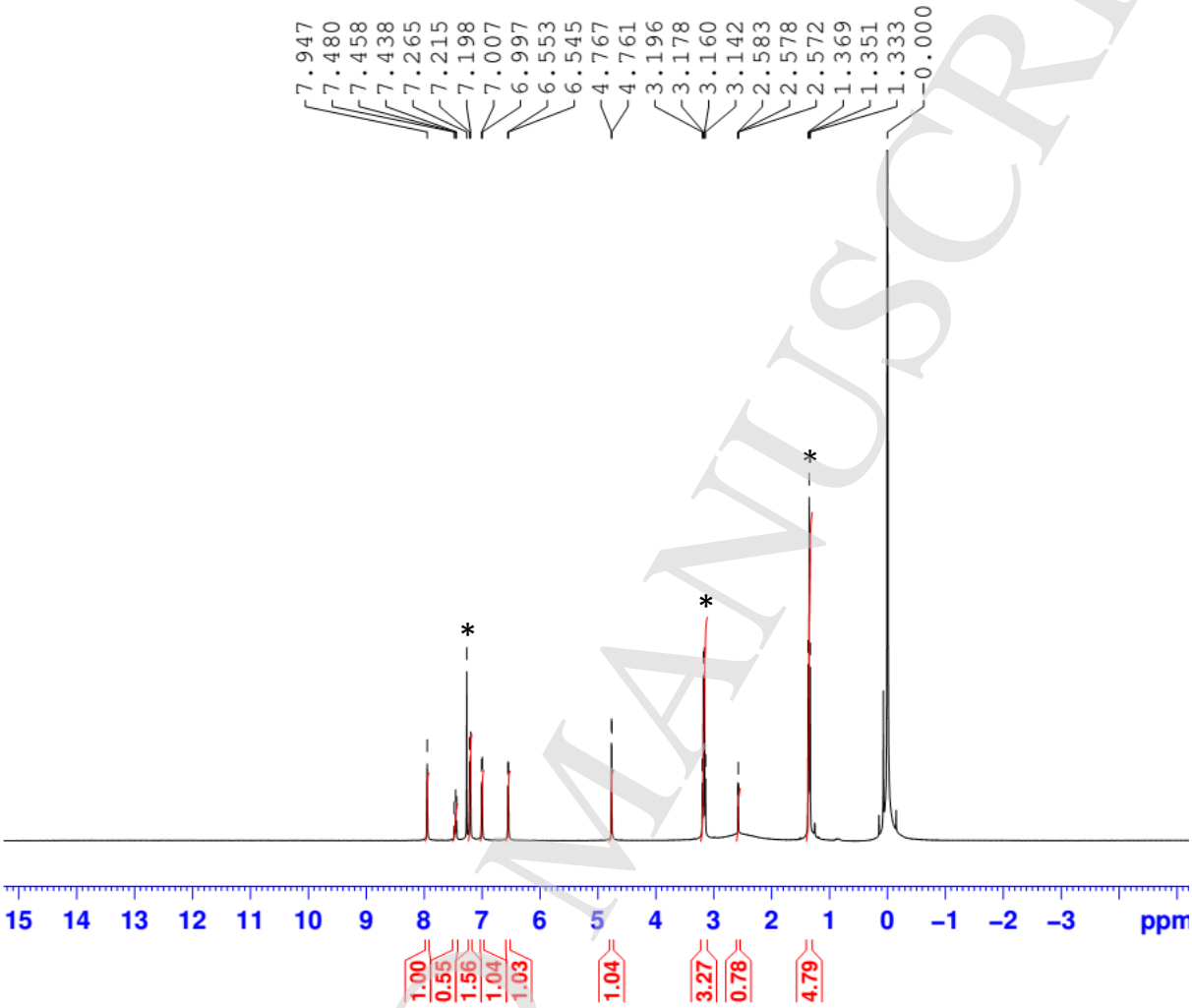

Figure S7 ^{1}H NMR spectrum of compound **2b**

ACCEPTED MANUSCRIPT

J. Porphyrins Phthalocyanines Downloaded from www.worldscientific.com
by UNIVERSITY OF NEW ENGLAND on 04/25/20. Re-use and distribution is strictly not permitted, except for Open Access articles.

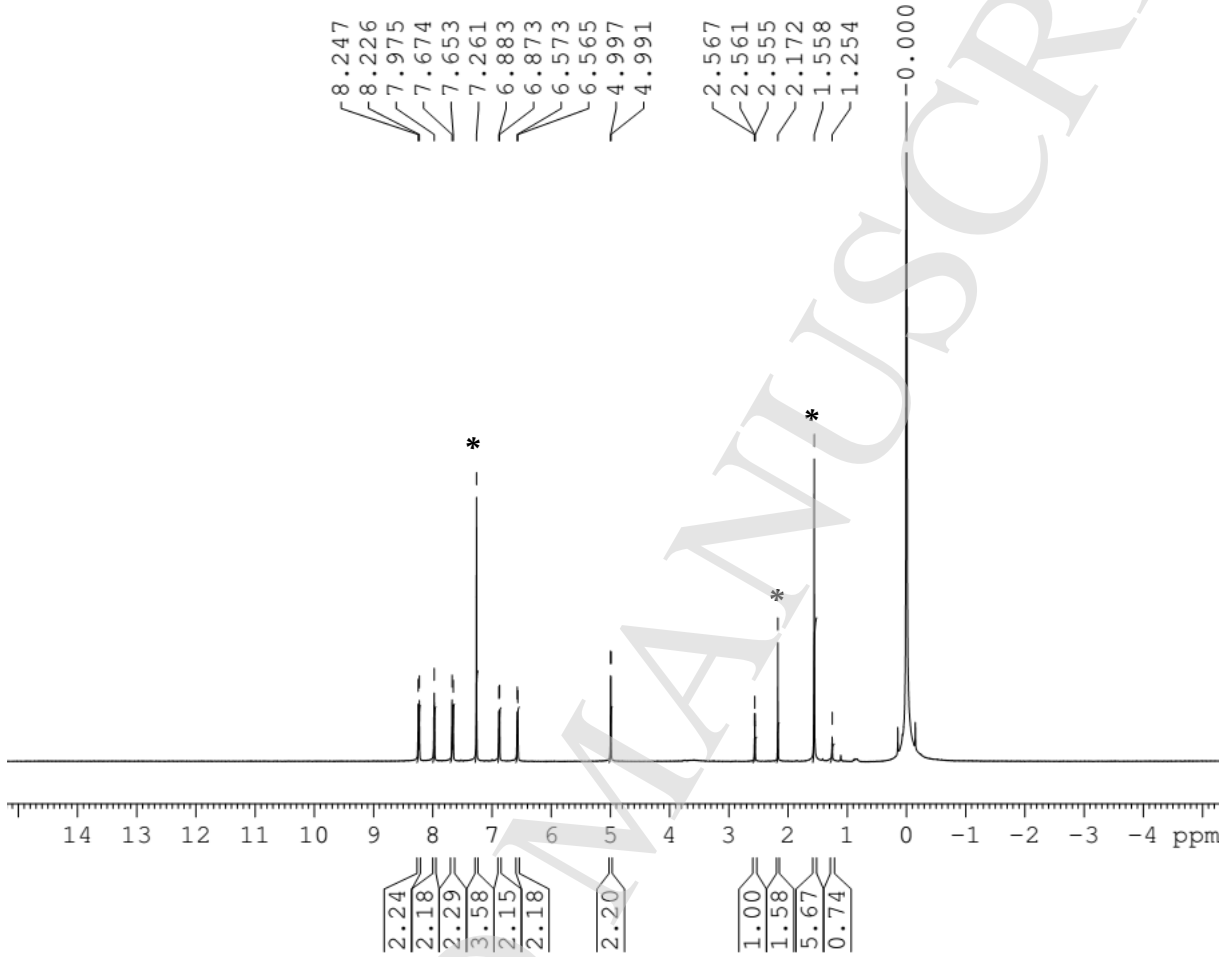

Figure S8 ^{1}H NMR spectrum of compound **3b**

ACCEPTED MANUSCRIPT

J. Porphyrins Phthalocyanines Downloaded from www.worldscientific.com
by UNIVERSITY OF NEW ENGLAND on 04/25/20. Re-use and distribution is strictly not permitted, except for Open Access articles.

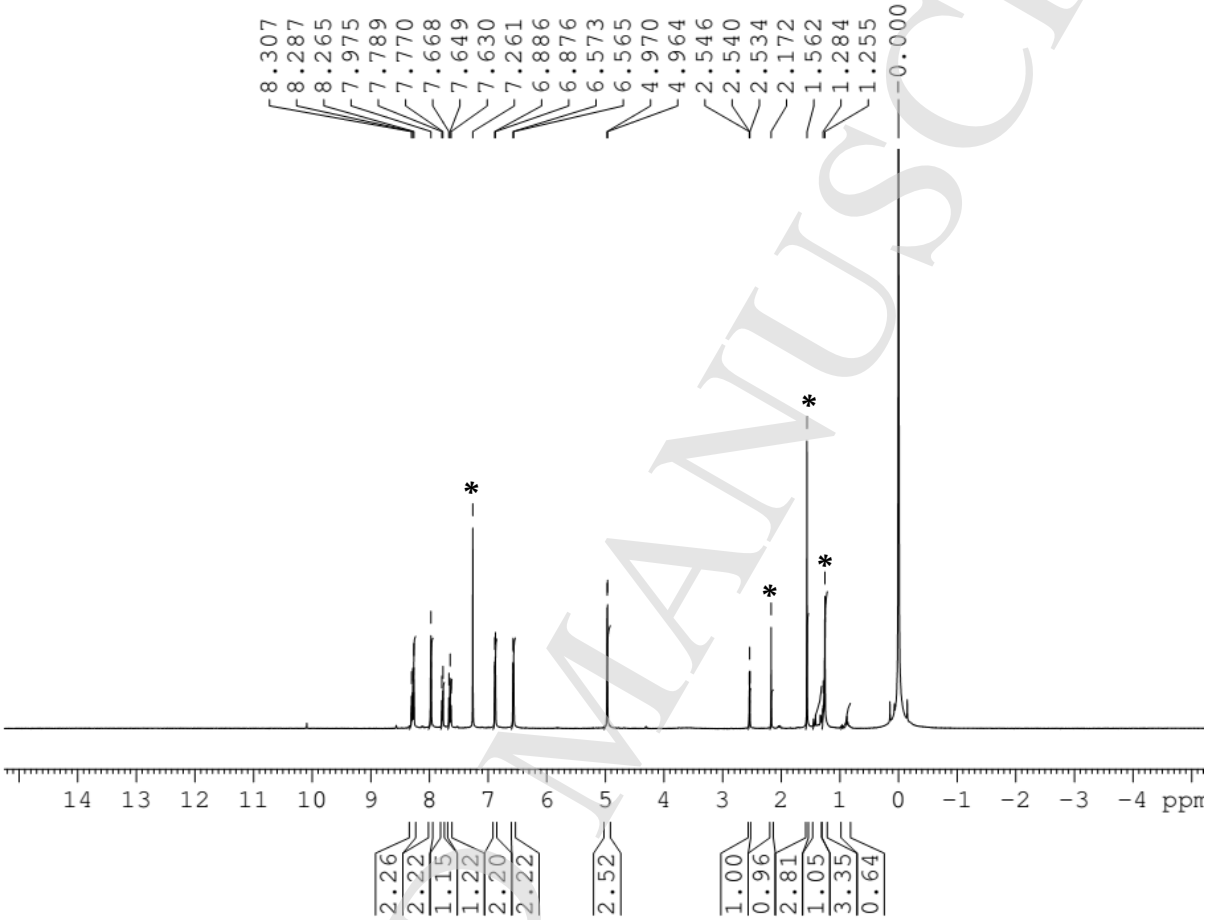

Figure S9 ^{1}H NMR spectrum of compound **4b**

ACCEPTED MANUSCRIPT

J. Porphyrins Phthalocyanines Downloaded from www.worldscientific.com
by UNIVERSITY OF NEW ENGLAND on 04/25/20. Re-use and distribution is strictly not permitted, except for Open Access articles.

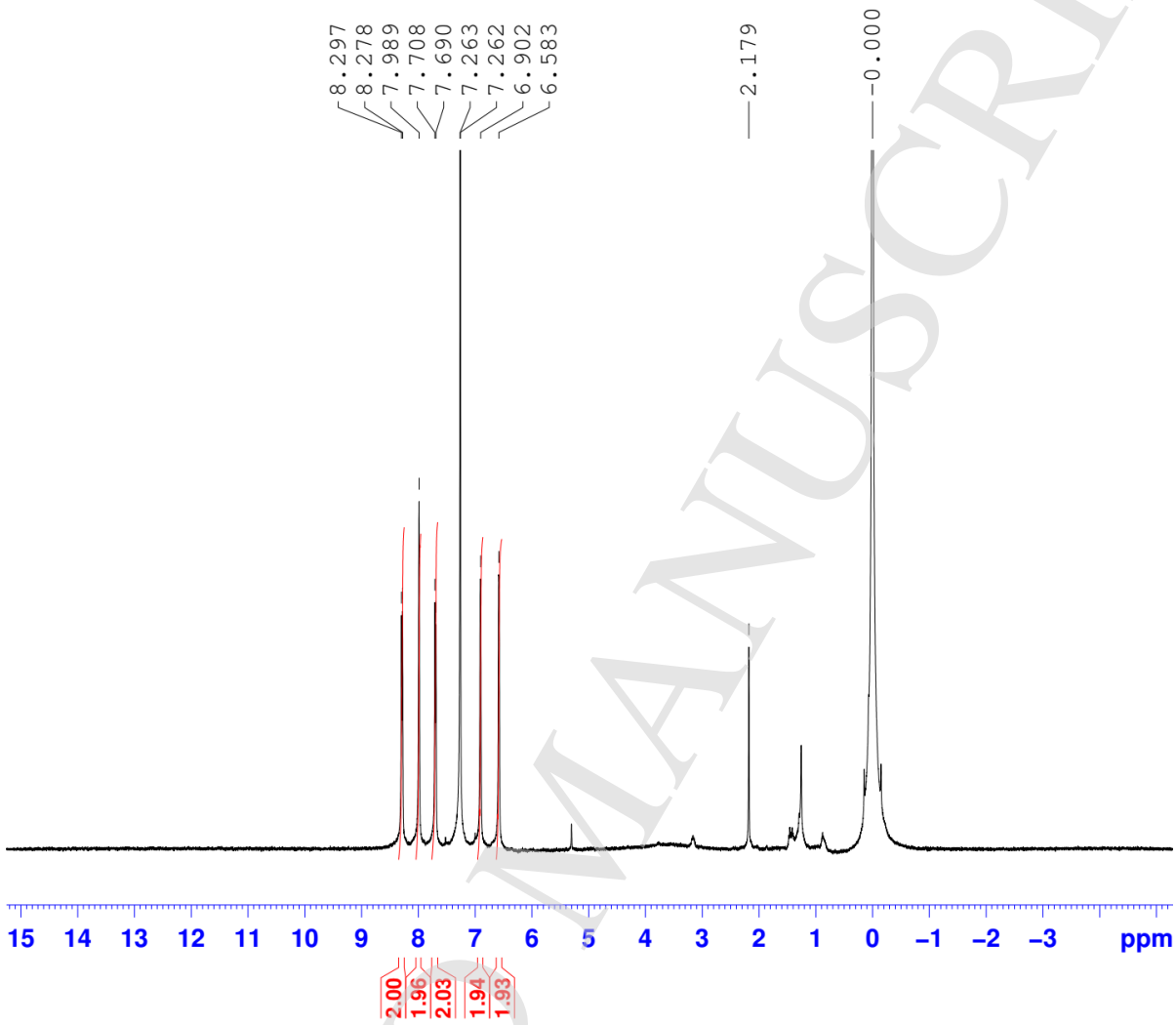

Figure S10 ^{1}H NMR spectrum of compound **5b**

ACCEPTED MANUSCRIPT

J. Porphyrins Phthalocyanines Downloaded from www.worldscientific.com
by UNIVERSITY OF NEW ENGLAND on 04/25/20. Re-use and distribution is strictly not permitted, except for Open Access articles.

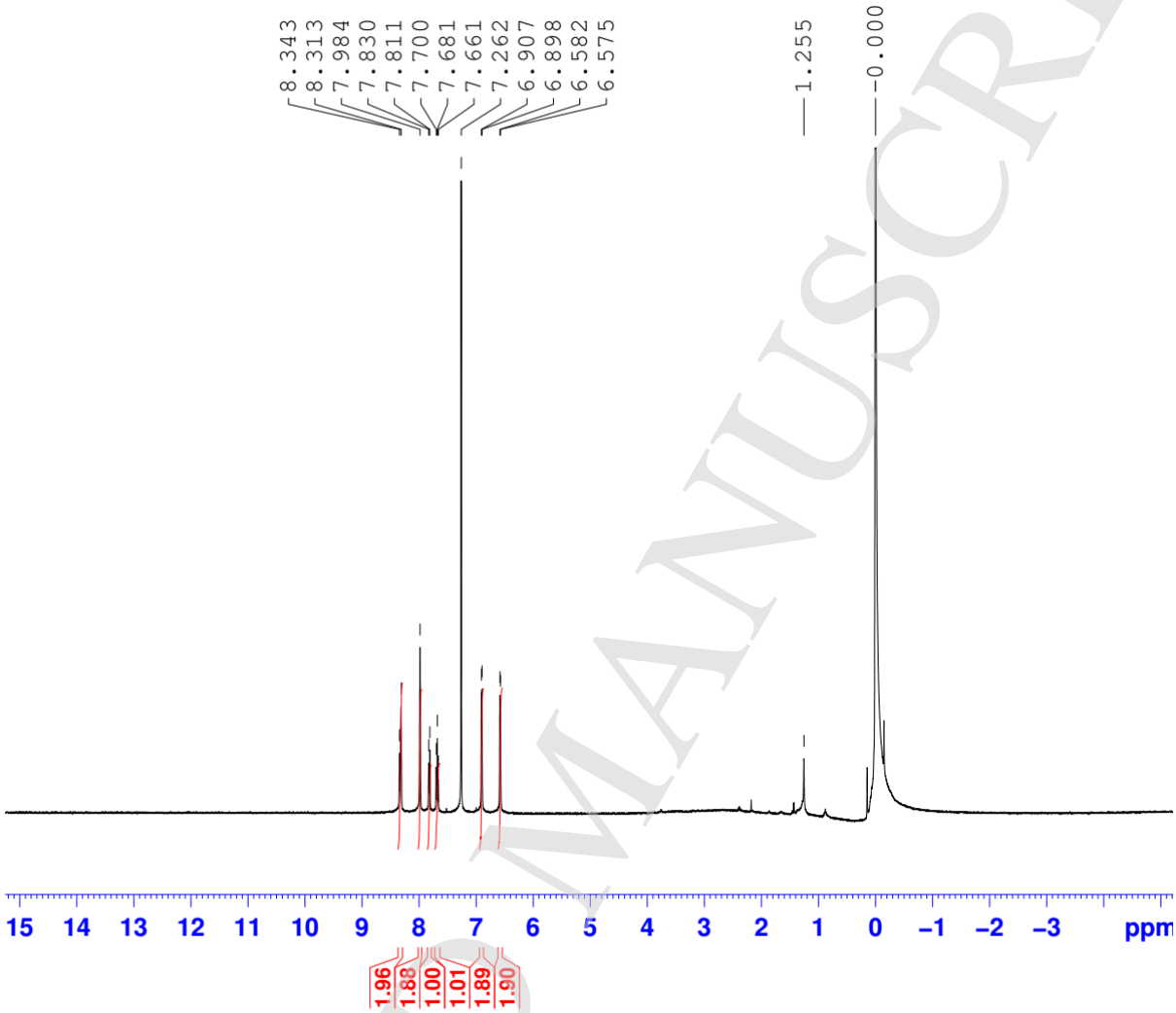

Figure S11 ^{1}H NMR spectrum of compound **6b**

ACCEPTED MANUSCRIPT

J. Porphyrins Phthalocyanines Downloaded from www.worldscientific.com
by UNIVERSITY OF NEW ENGLAND on 04/25/20. Re-use and distribution is strictly not permitted, except for Open Access articles.

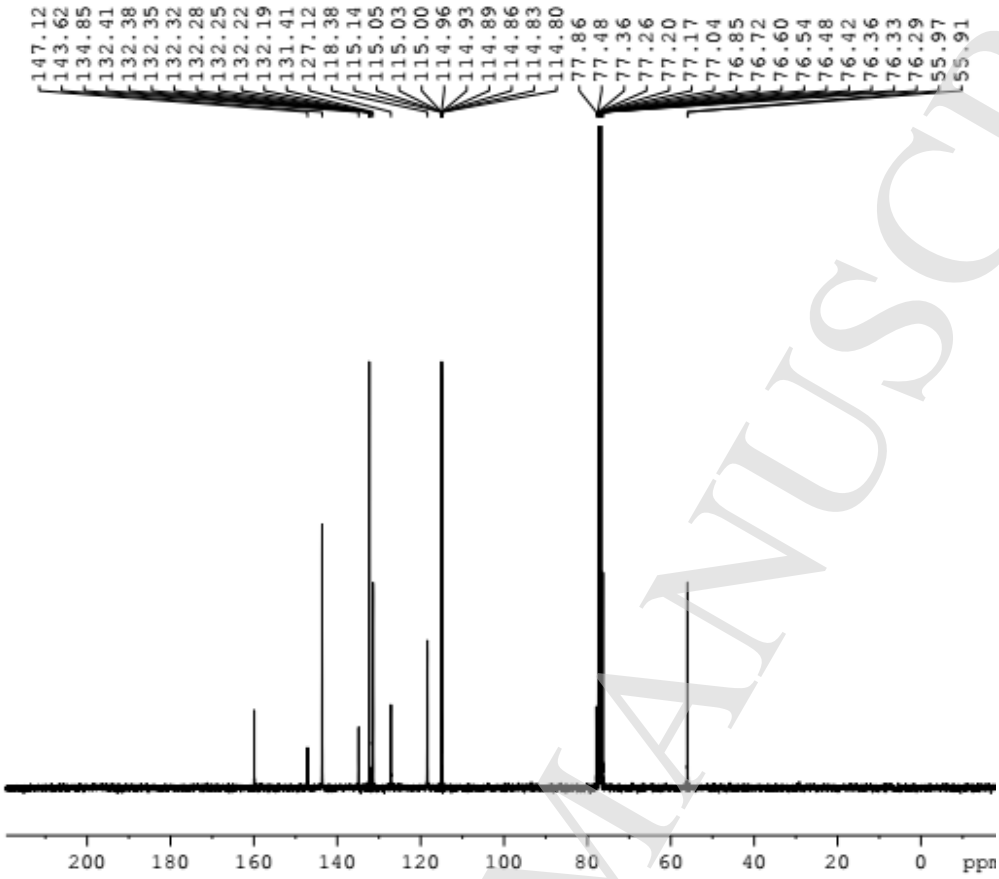

Figure S12 C-13 NMR spectrum of compound **1b**

ACCEPTED MANUSCRIPT

J. Porphyrins Phthalocyanines Downloaded from www.worldscientific.com
by UNIVERSITY OF NEW ENGLAND on 04/25/20. Re-use and distribution is strictly not permitted, except for Open Access articles.

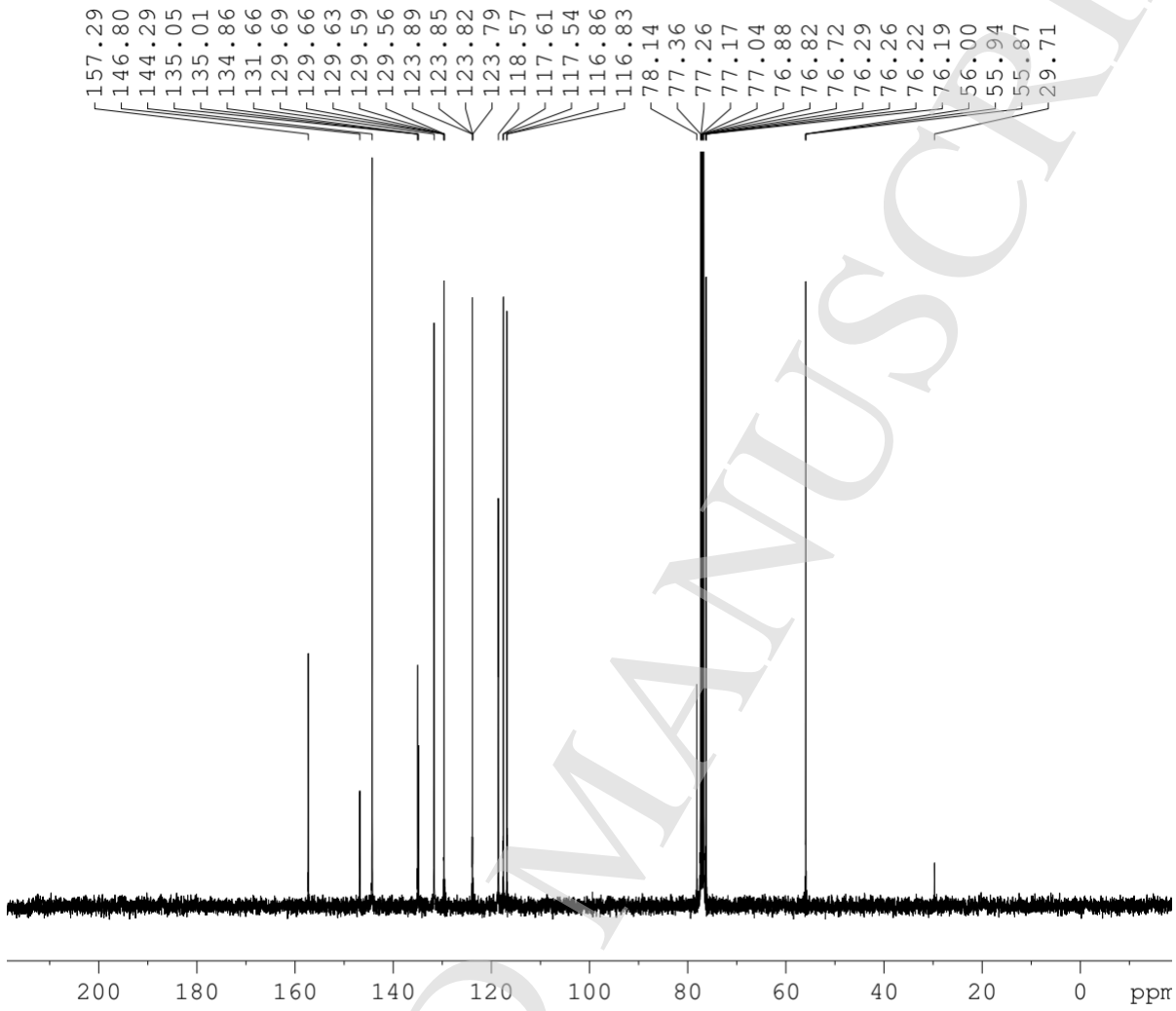

Figure S13 C-13 NMR spectrum of compound **2b**

ACCEPTED MANUSCRIPT

J. Porphyrins Phthalocyanines Downloaded from www.worldscientific.com
by UNIVERSITY OF NEW ENGLAND on 04/25/20. Re-use and distribution is strictly not permitted, except for Open Access articles.

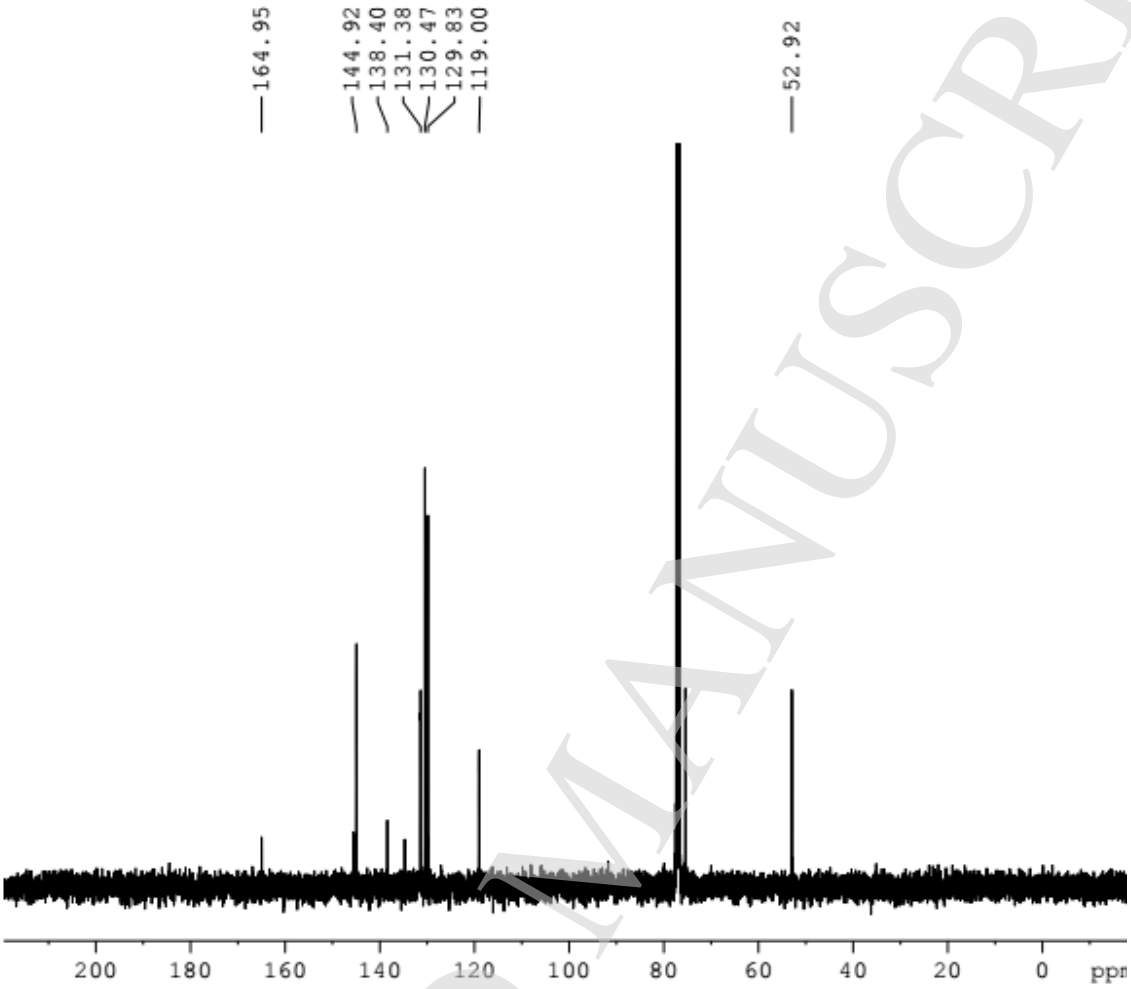

Figure S13 C-13 NMR spectrum of compound **3b**

ACCEPTED MANUSCRIPT

J. Porphyrins Phthalocyanines Downloaded from www.worldscientific.com
by UNIVERSITY OF NEW ENGLAND on 04/25/20. Re-use and distribution is strictly not permitted, except for Open Access articles.

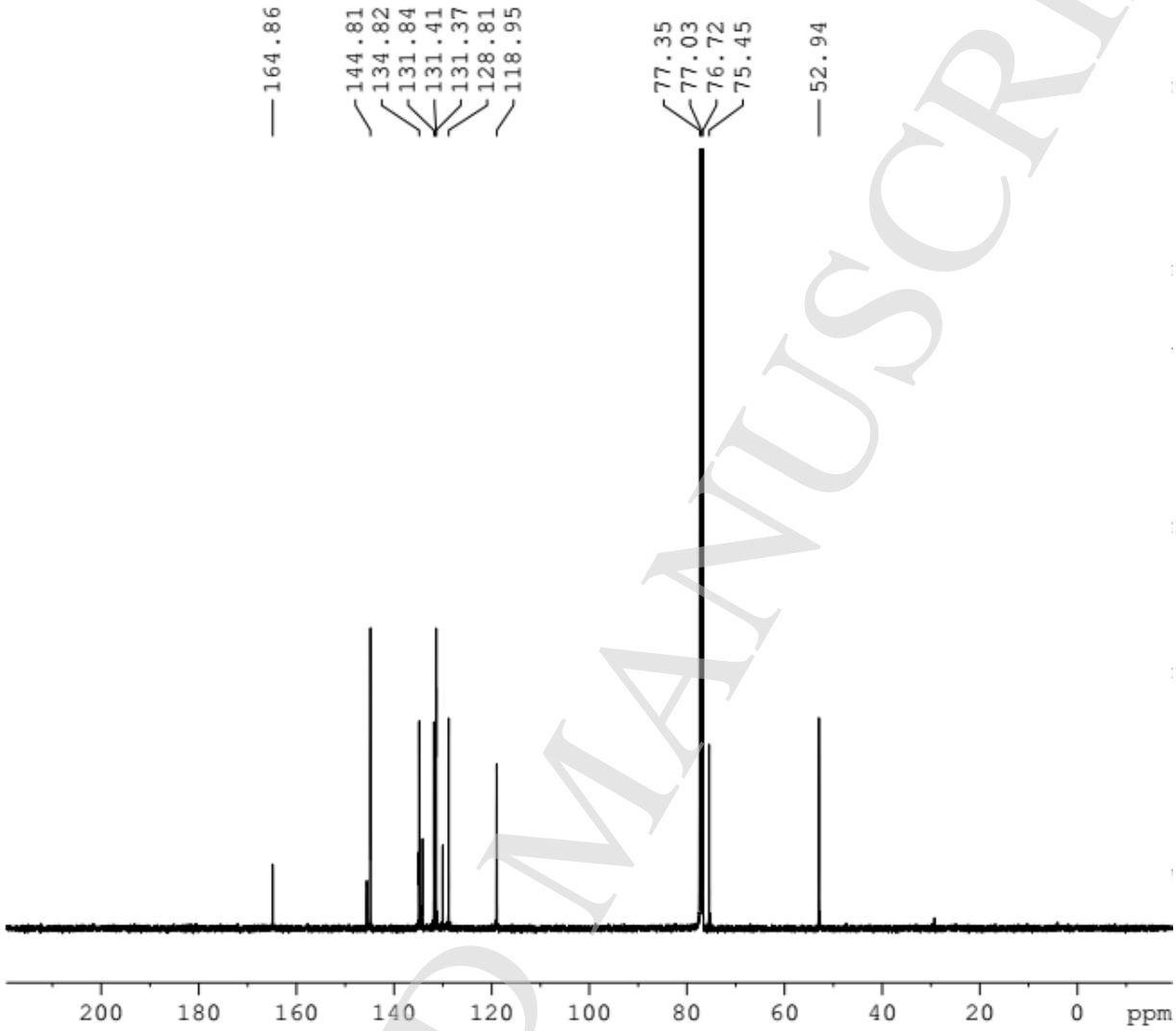

Figure S14 C-13 NMR spectrum of compound **4b**

ACCEPTED MANUSCRIPT

J. Porphyrins Phthalocyanines Downloaded from www.worldscientific.com
by UNIVERSITY OF NEW ENGLAND on 04/25/20. Re-use and distribution is strictly not permitted, except for Open Access articles.

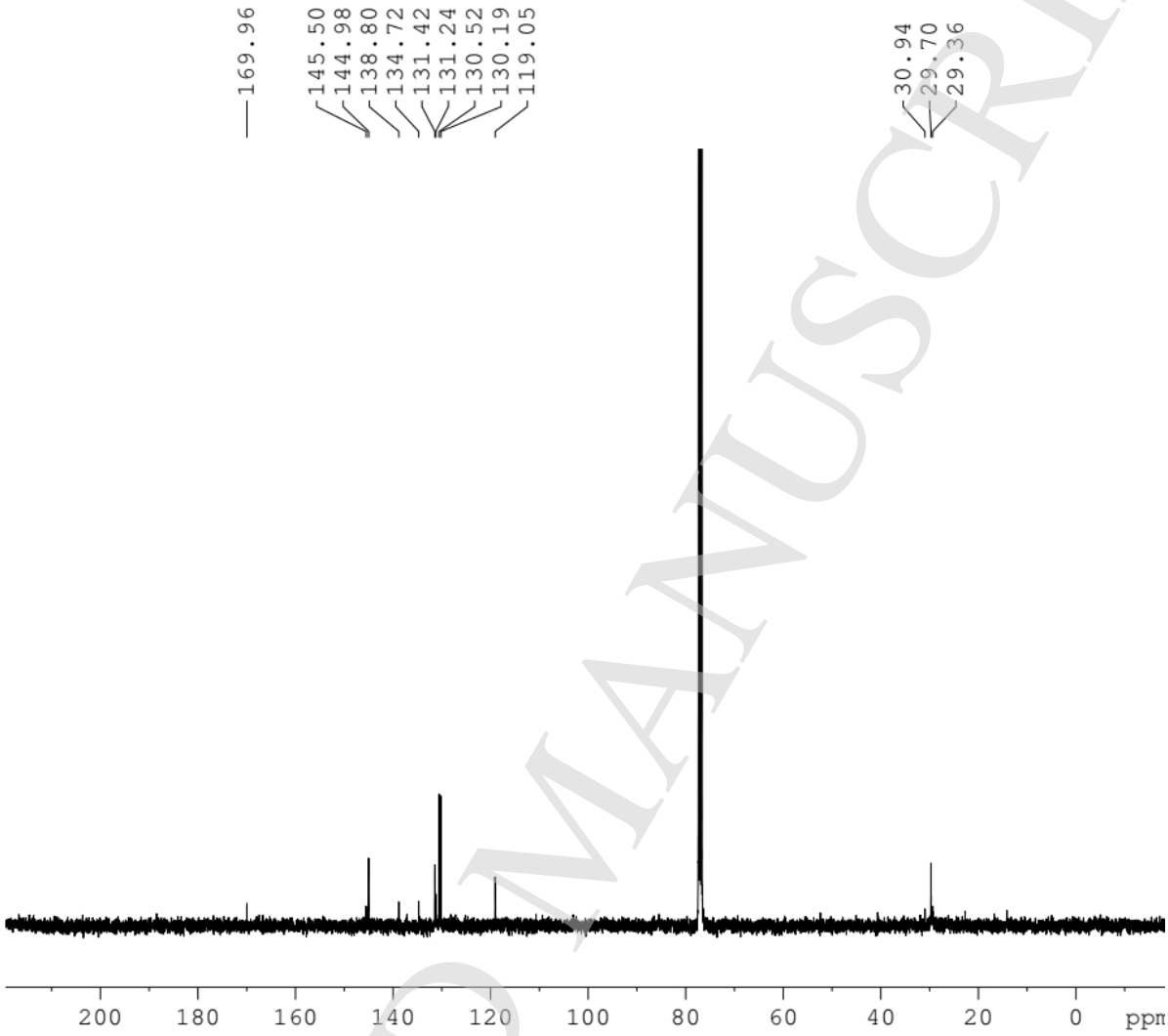

Figure S15 C-13 NMR spectrum of compound **5b**

ACCEPTED MANUSCRIPT

J. Porphyrins Phthalocyanines Downloaded from www.worldscientific.com
by UNIVERSITY OF NEW ENGLAND on 04/25/20. Re-use and distribution is strictly not permitted, except for Open Access articles.

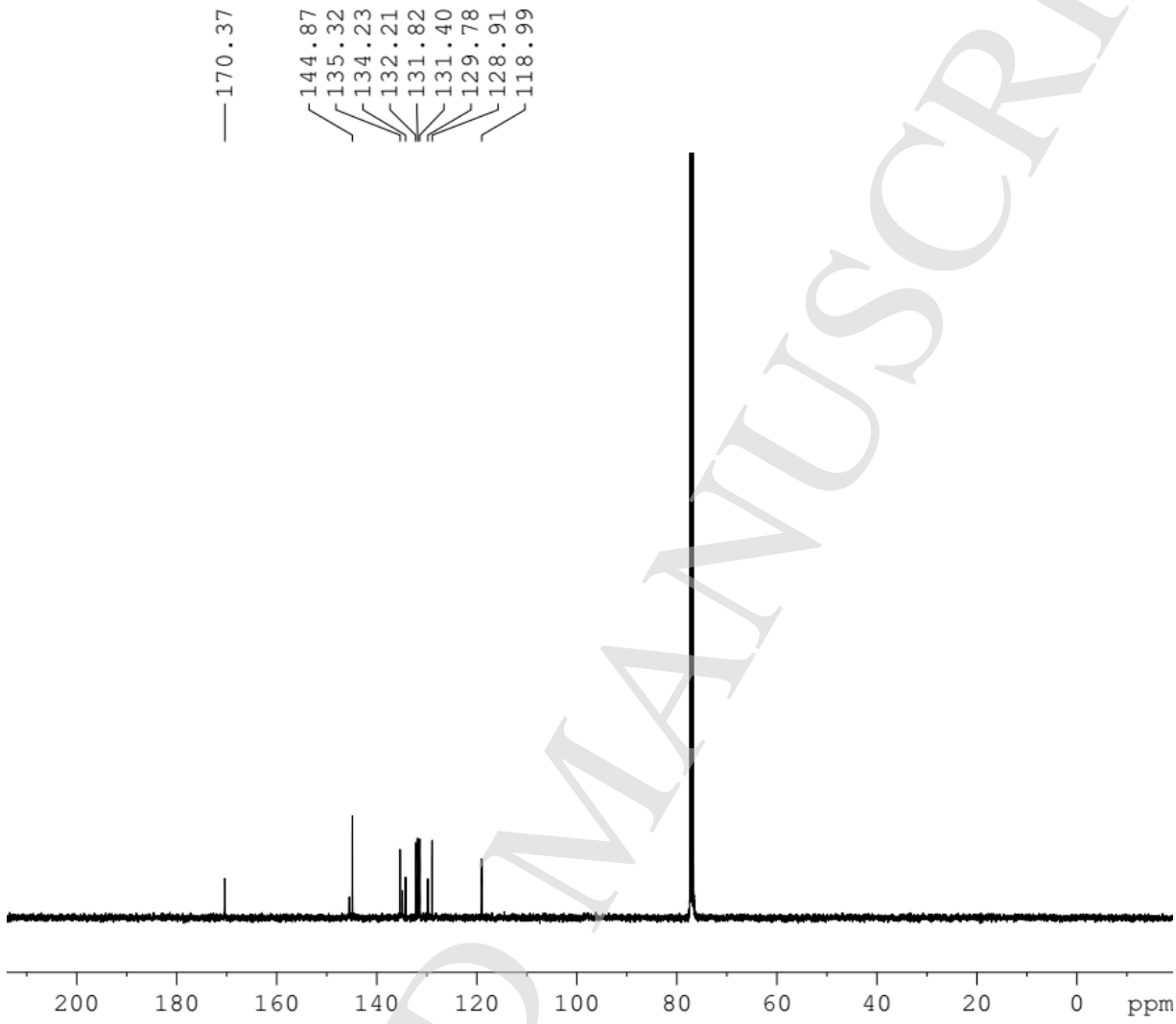

Figure S16. C-13 NMR spectrum of compound **6b**

ACCEPTED MANUSCRIPT

J. Porphyrins Phthalocyanines Downloaded from www.worldscientific.com
by UNIVERSITY OF NEW ENGLAND on 04/25/20. Re-use and distribution is strictly not permitted, except for Open Access articles.

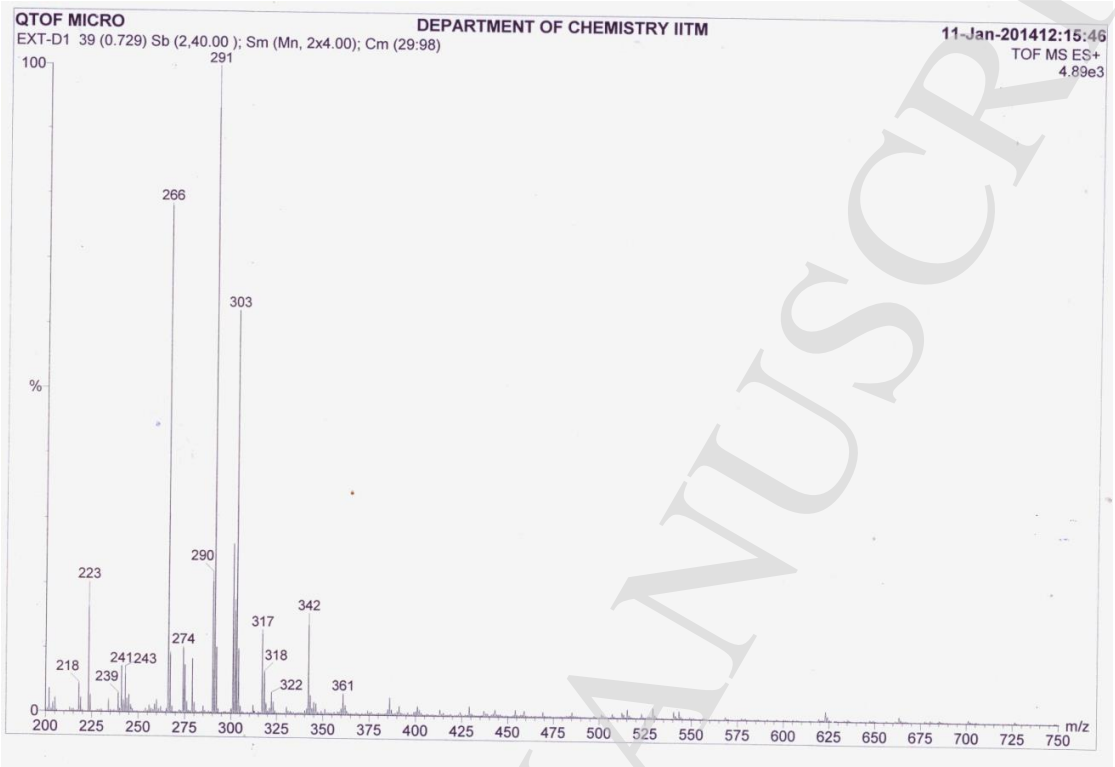

Figure S17. Mass spectrum of compound **1b**

ACCEPTED MANUSCRIPT

J. Porphyrins Phthalocyanines Downloaded from www.worldscientific.com
by UNIVERSITY OF NEW ENGLAND on 04/25/20. Re-use and distribution is strictly not permitted, except for Open Access articles.

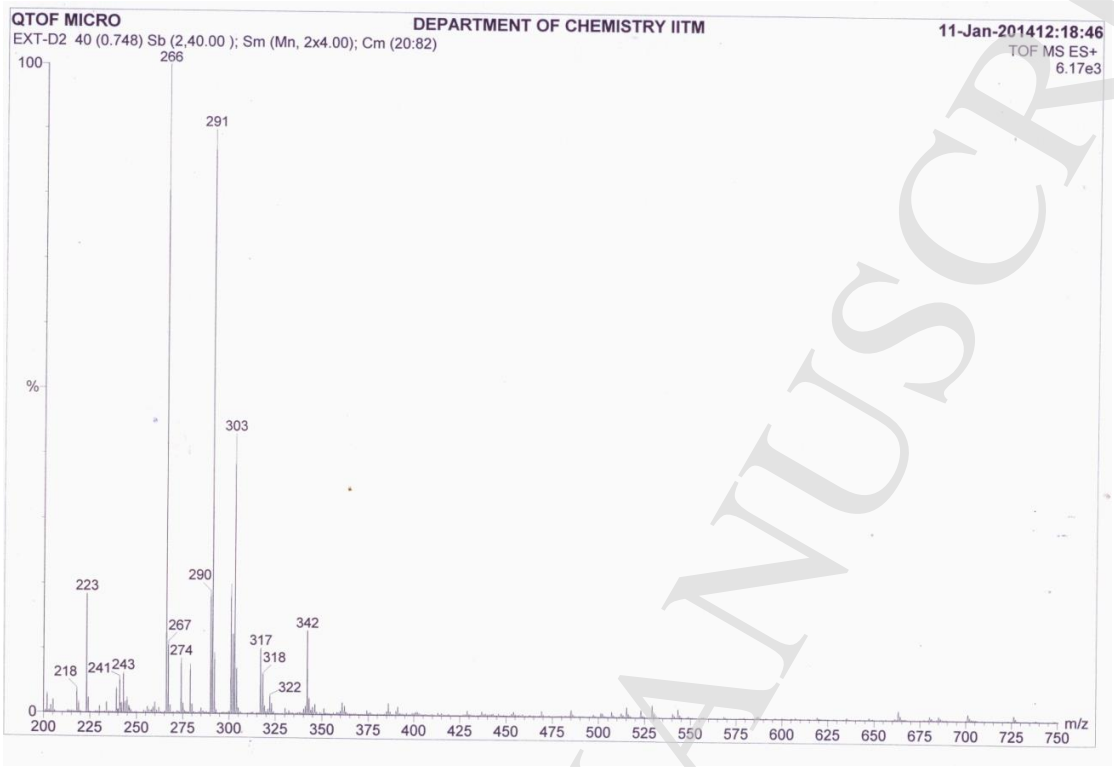

Figure S18. Mass spectrum of compound **2b**

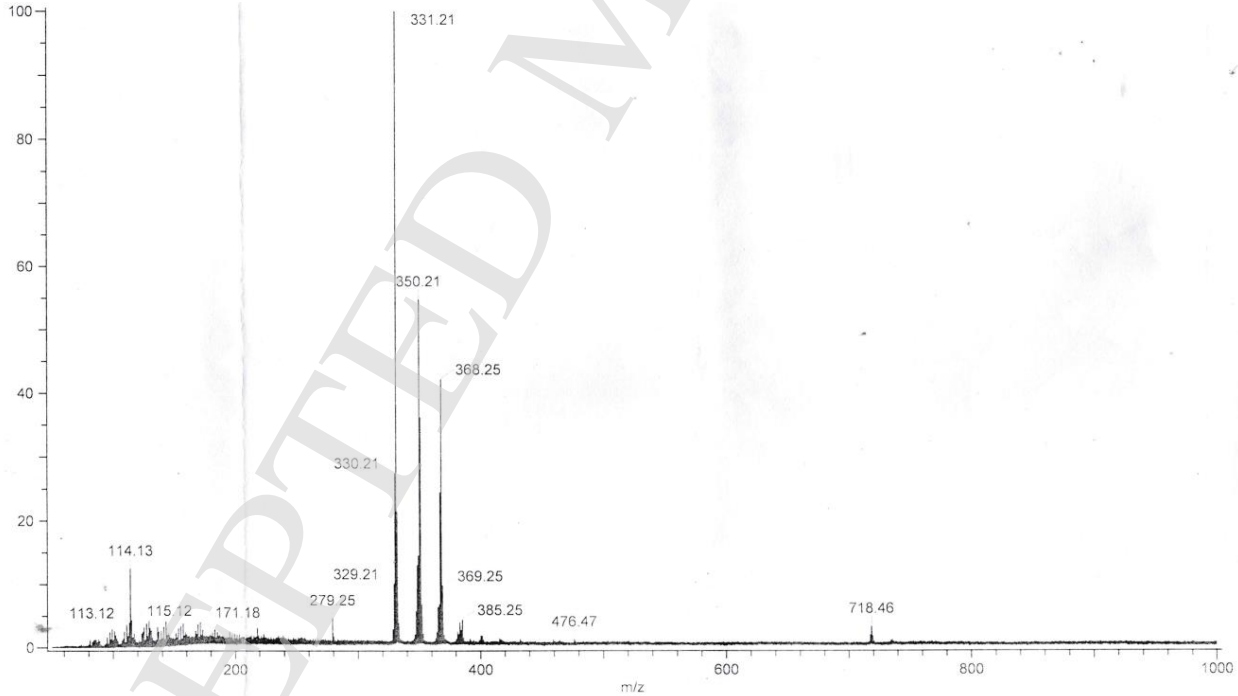

Figure S19. Mass spectrum of compound **3b**

ACCEPTED MANUSCRIPT

J. Porphyrins Phthalocyanines Downloaded from www.worldscientific.com
by UNIVERSITY OF NEW ENGLAND on 04/25/20. Re-use and distribution is strictly not permitted, except for Open Access articles.

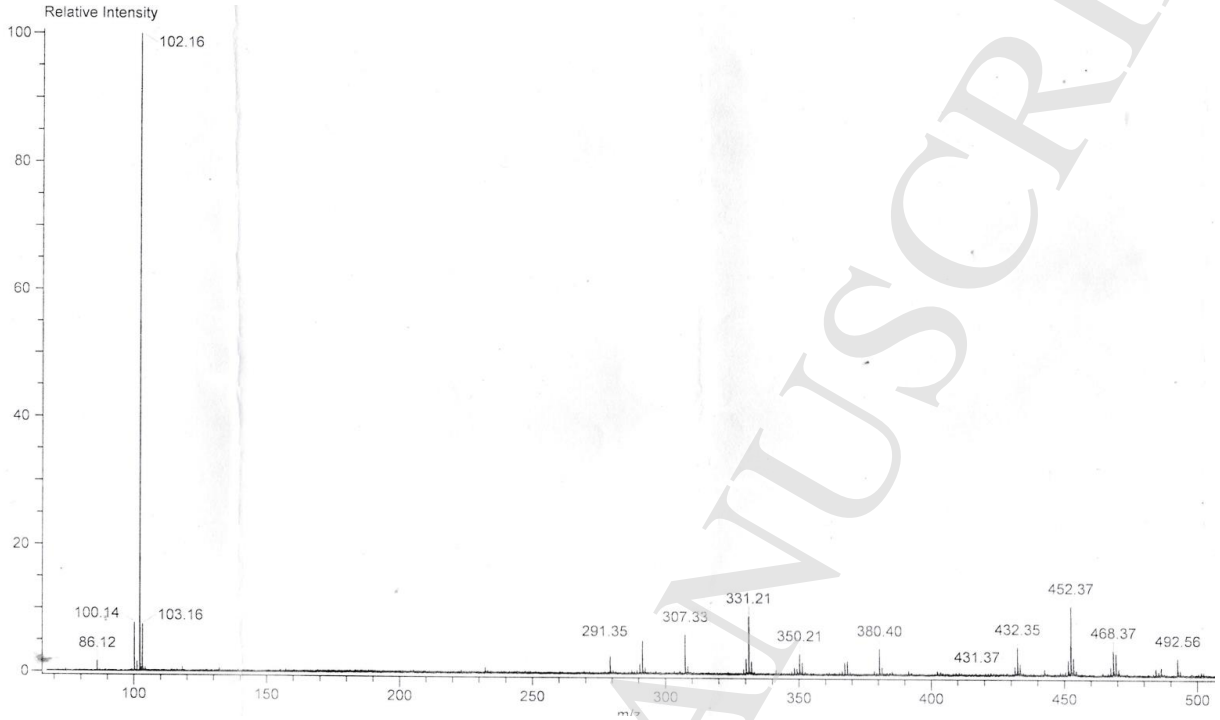

Figure S20. Mass spectrum of compound **4b**

ACCEPTED MANUSCRIPT

J. Porphyrins Phthalocyanines Downloaded from www.worldscientific.com
by UNIVERSITY OF NEW ENGLAND on 04/25/20. Re-use and distribution is strictly not permitted, except for Open Access articles.

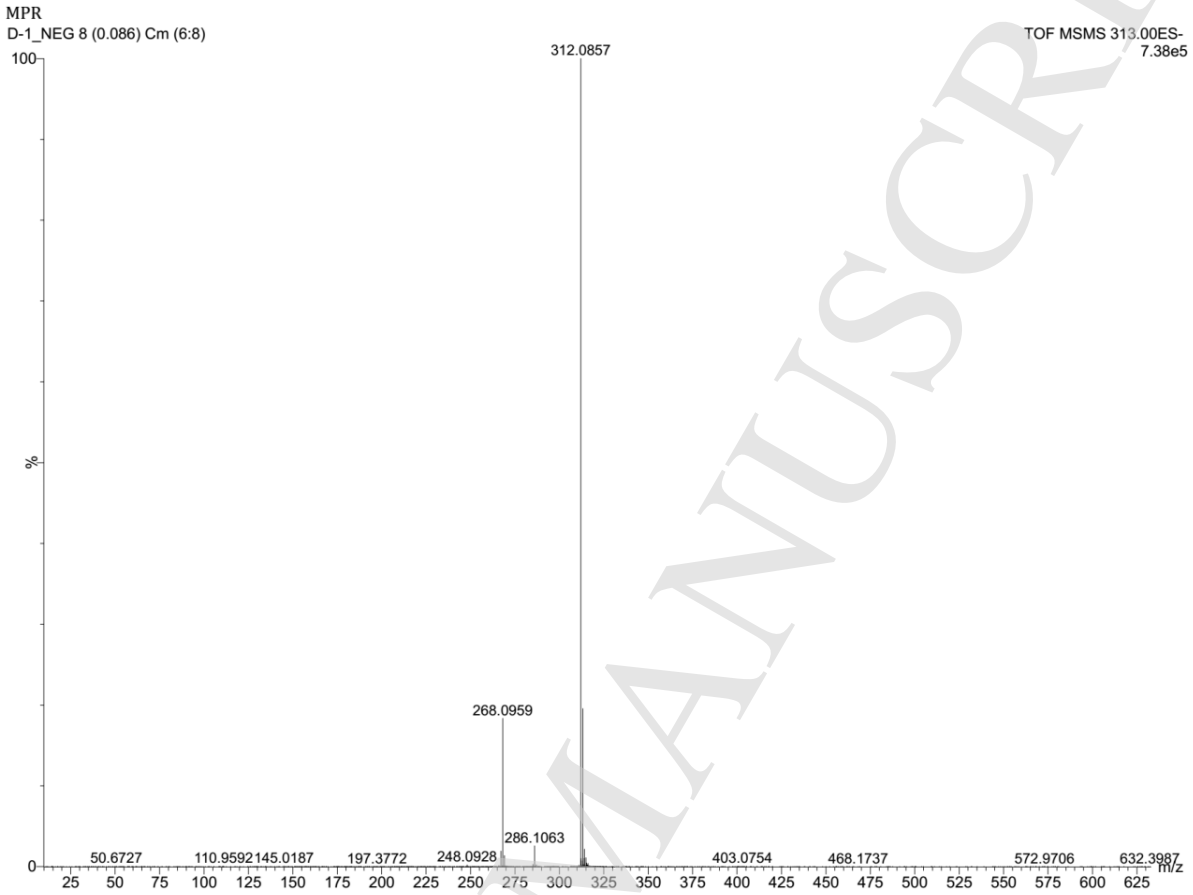

Figure S21. Mass spectrum of compound **5b**

ACCEPTED MANUSCRIPT

J. Porphyrins Phthalocyanines Downloaded from www.worldscientific.com
by UNIVERSITY OF NEW ENGLAND on 04/25/20. Re-use and distribution is strictly not permitted, except for Open Access articles.

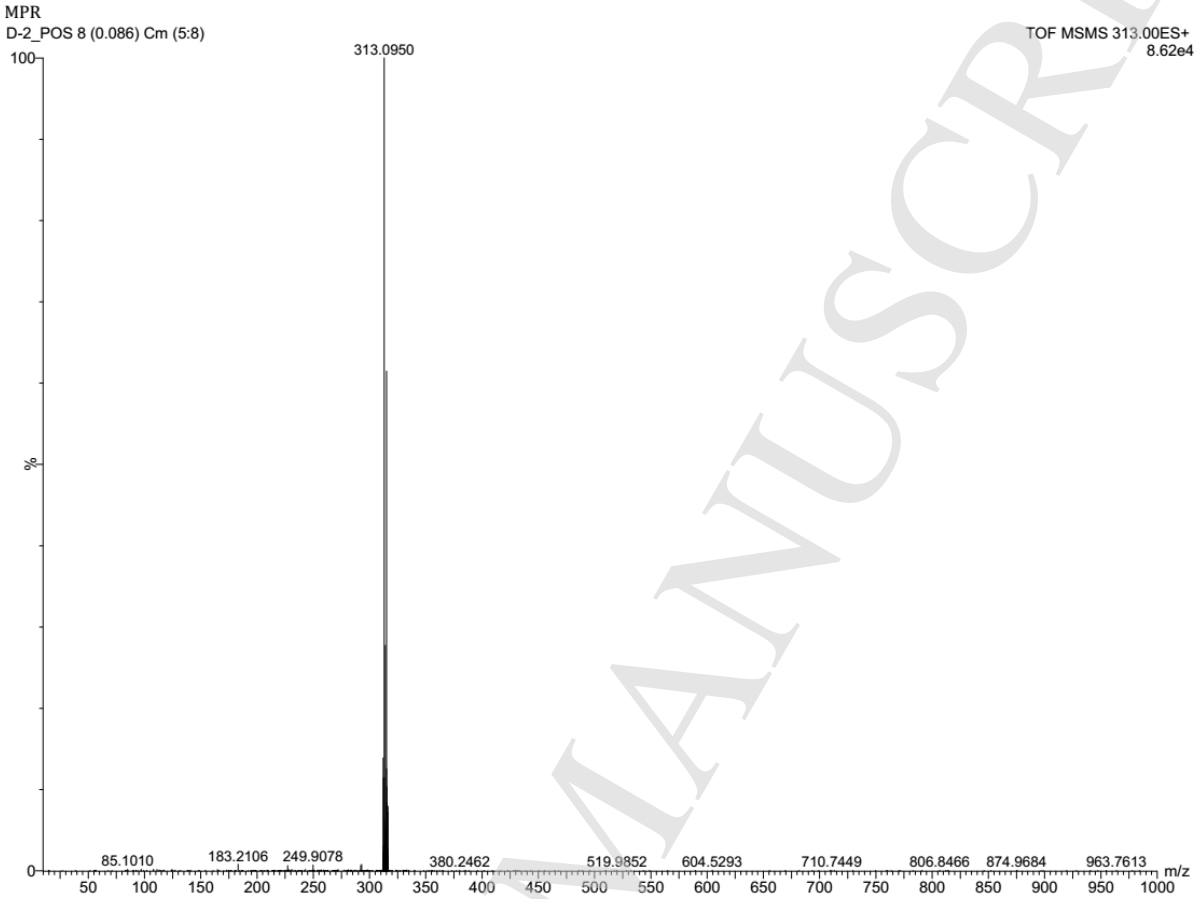

Figure S22. Mass spectrum of compound **6b**

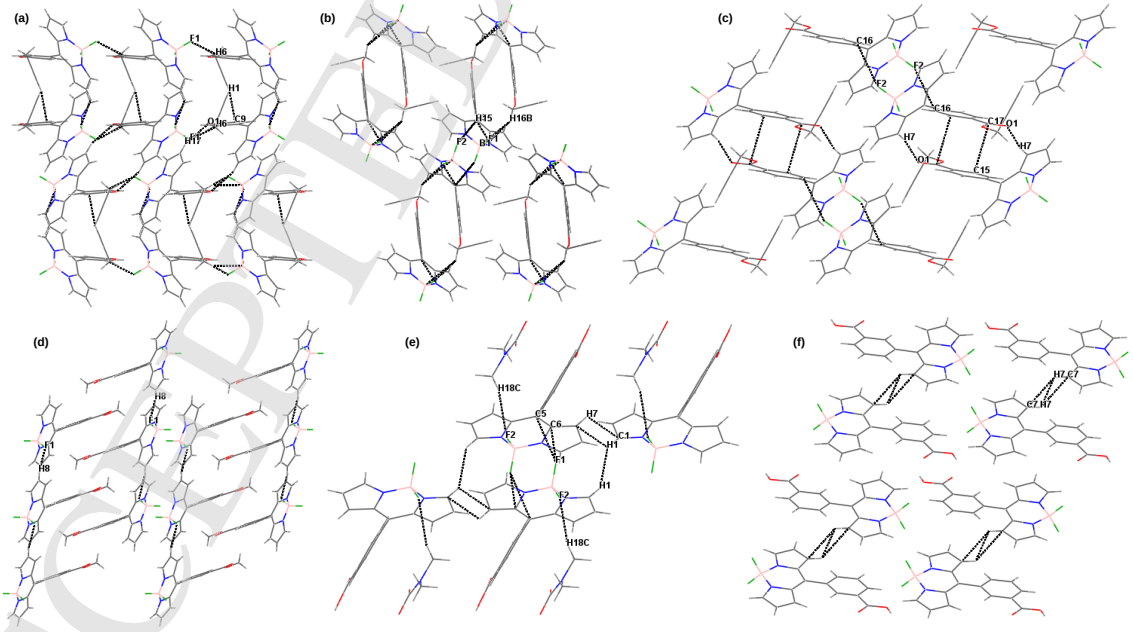

ACCEPTED MANUSCRIPT

Figure S23. Packing diagrams of (a) **1b**, viewed down 'c' axis; (b) **2b**, viewed along 'a' axis; (c) **3b**, viewed along 'b' axis; (d) **4b**, viewed along 'b' axis; (e) **5b**, viewed down 'a' axis and (f) **6b**, viewed along 'a' axis.

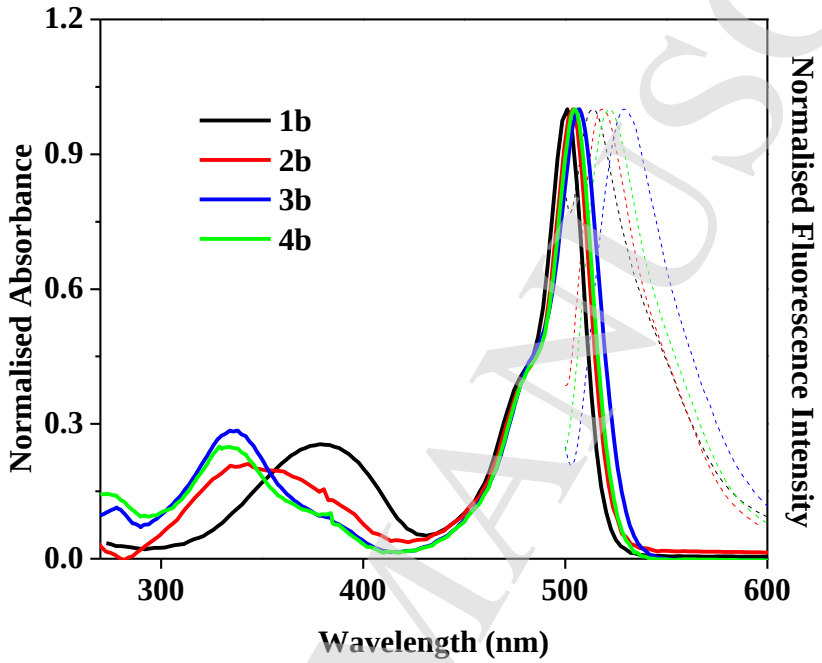

Figure S24. Normalized UV-Visible (solid) and fluorescence (dash) spectra of compounds, **1b**-**4b**.

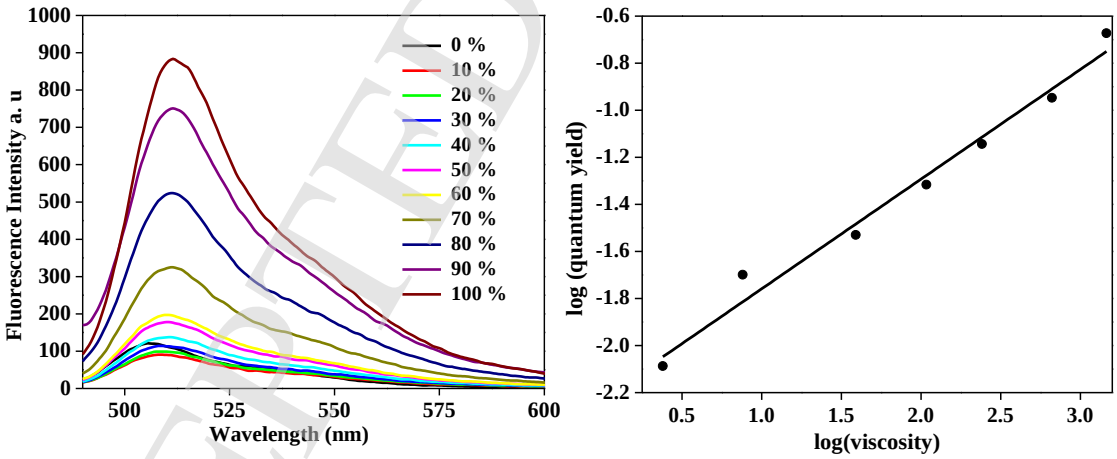

Figure S25. (a) Fluorescence intensity *versus* wavelength (b) log (quantum yield) *versus* log (viscosity) for compound **1b**.

J. Porphyrins Phthalocyanines Downloaded from www.worldscientific.com
by UNIVERSITY OF NEW ENGLAND on 04/25/20. Re-use and distribution is strictly not permitted, except for Open Access articles.

ACCEPTED MANUSCRIPT

J. Porphyrins Phthalocyanines Downloaded from www.worldscientific.com
by UNIVERSITY OF NEW ENGLAND on 04/25/20. Re-use and distribution is strictly not permitted, except for Open Access articles.

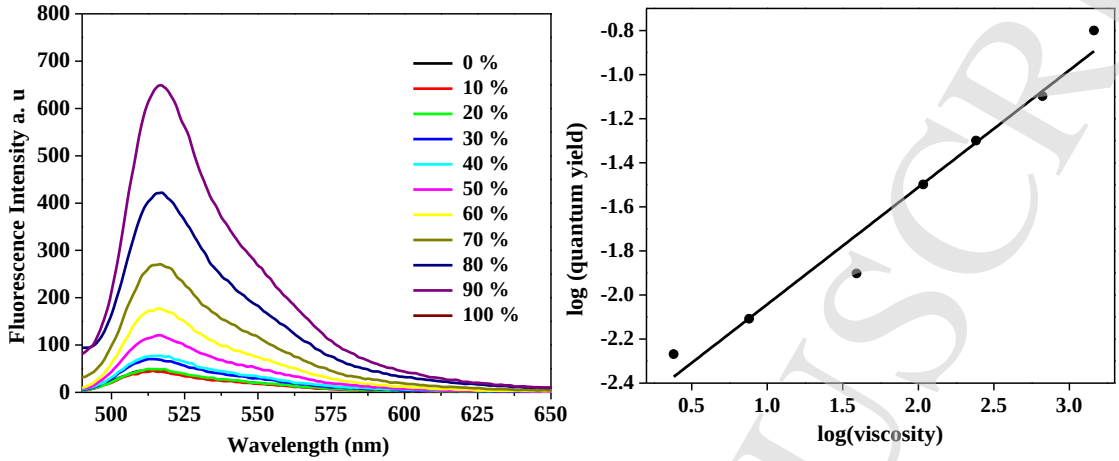

Figure S26. (a) Fluorescence intensity *versus* wavelength (b) log (quantum yield) *versus* log (viscosity) for compound **2b**.

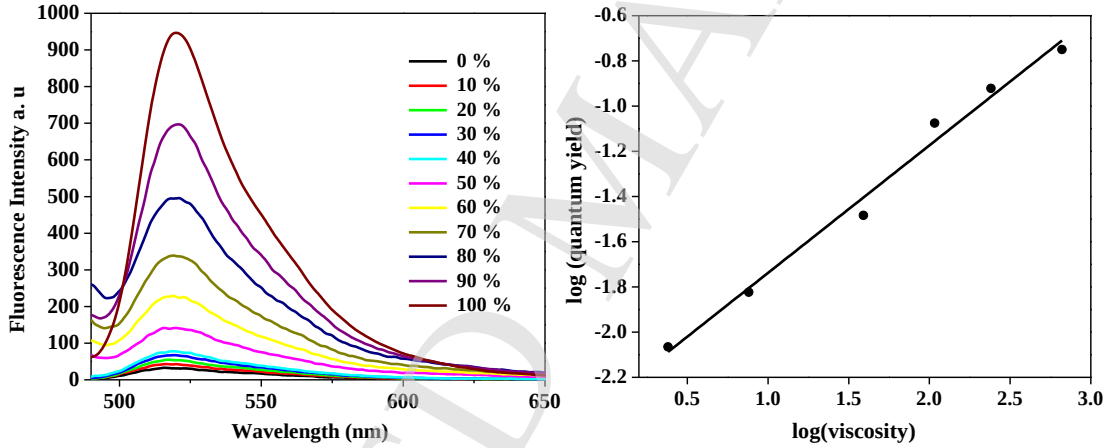

Figure S27. (a) Fluorescence intensity *versus* wavelength (b) log (quantum yield) *versus* log (viscosity) for compound **4b**.

ACCEPTED MANUSCRIPT

J. Porphyrins Phthalocyanines Downloaded from www.worldscientific.com
by UNIVERSITY OF NEW ENGLAND on 04/25/20. Re-use and distribution is strictly not permitted, except for Open Access articles.

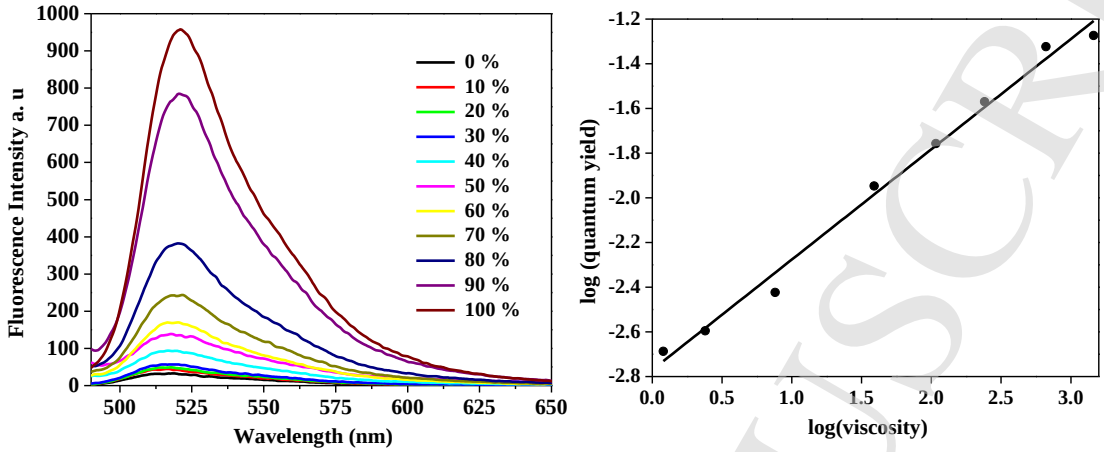

Figure S28. (a) Fluorescence intensity *versus* wavelength (b) log (quantum yield) *versus* log (viscosity) for compound **5b**.

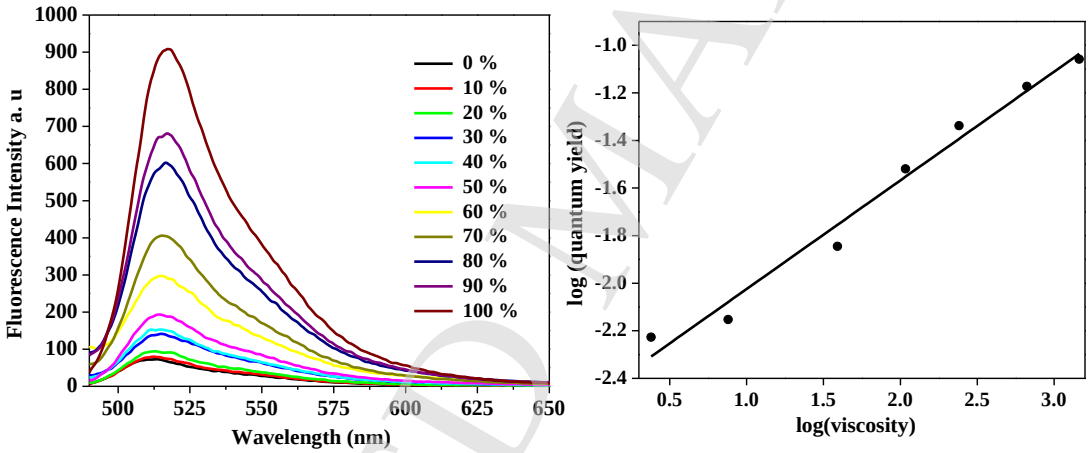

Figure S29. (a) Fluorescence intensity *versus* wavelength (b) log (quantum yield) *versus* log (viscosity) for compound **6b**.

ACCEPTED MANUSCRIPT

J. Porphyrins Phthalocyanines Downloaded from www.worldscientific.com
by UNIVERSITY OF NEW ENGLAND on 04/25/20. Re-use and distribution is strictly not permitted, except for Open Access articles.

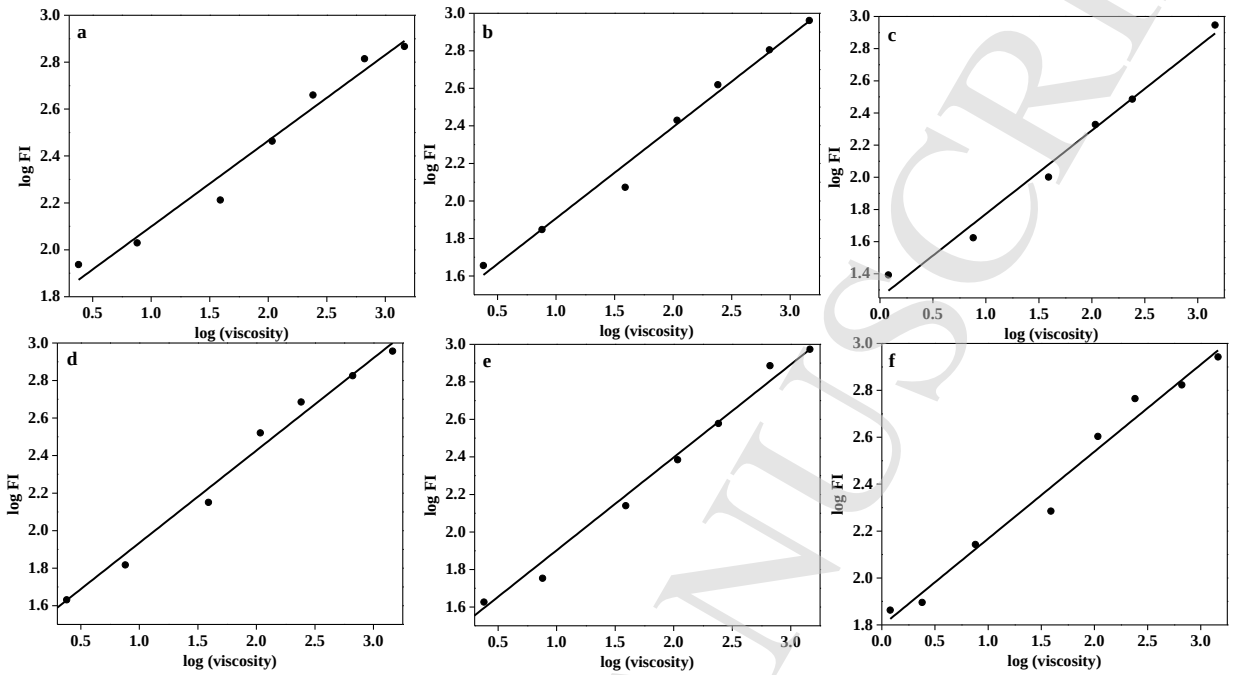

Figure S30. Log FI *versus* log viscosity of (a) **1b** (b) **2b** (c) **3b** (d) **4b** (e) **5b** (f) **6b**.

Table S1. Electrochemical redox data of BODIPYs, **1b-6b**.

Code	Reduction potential (V)	
	I	II
1b	-0.89	-1.86
2b	-0.82	-1.74
3b	-0.74	-1.40
4b	-0.78	-1.66
5b	-0.77	-1.76
6b	-0.81	-1.87

Table S2. Crystallographic data of compounds, **1b-6b**.

	1b	**2b**	**3b**	**4b**	**5b**	**6b**
Empirical formula	$C_{18}H_{13}BF_2N_2O$	$C_{18}H_{13}BF_2N_2O$	$C_{19}H_{13}BF_2N_2O_2$	$C_{19}H_{13}BF_2N_2O_2$	$C_{19}H_{18}BF_2N_3O_3$	$C_{16}H_{11}BF_2N_2O_2$
fw	322.11	322.11	350.12	350.12	385.17	312.08
CCDC	948480	974214	998567	998566	1041761	1058015
Colour	Reddish orange	Reddish orange	Reddish orange	Reddish orange	Red	Red
Crystal system	Monoclinic	Triclinic	Monoclinic	Triclinic	Triclinic	Triclinic
Space Group	$P2_1/c$	P-1	C 2/c	P-1	P-1	P-1
a (Å)	7.9143(3)	7.5655(3)	18.4570(8)	7.598(5)	7.5675(4)	6.3235(3)
b (Å)	22.2208(7)	9.2713(4)	8.1338(3)	8.228(5)	8.0165(5)	10.9748(6)
c (Å)	9.0858(3)	12.2205(6)	23.8102(10)	14.250(5)	16.2954(11)	11.2670(7)

ACCEPTED MANUSCRIPT

J. Porphyrins Phthalocyanines Downloaded from www.worldscientific.com
by UNIVERSITY OF NEW ENGLAND on 04/25/20. Re-use and distribution is strictly not permitted, except for Open Access articles.

α (deg)	90	68.821(2)	90	106.634(5)	97.444(3)	109.676(3)
β (deg)	101.7830(10)	86.408(2)	111.793(1)	93.652(5)	99.645(3)	99.053(4)
γ (deg)	90	72.376(2)	90	102.831(5)	104.263(3)	99.609(3)
Volume (A^3)	1564.18(9)	760.71(6)	3319.1(2)	824.5(8)	929.32(10)	706.47(7)
Z	4	2	8	2	2	2
D_{calcd}(mg/m^3)	1.368	1.406	1.401	1.410	1.376	1.467
Wavelength (λ) Å	0.71073	0.71073	0.71073	0.71073	0.71073	0.71073
Temperature (K)	293(2)	293(2)	296(2)	293(2)	296(2)	296(2)
Data / restraints / parameters	2759 / 0 / 222	4414 / 0 / 218	3262/ 0 / 240	2894 / 0 / 240	4058 / 0 / 266	2492 / 0 / 209
F(000)	664	332	1440	360	400	320
GOF on F^2	1.052	1.043	1.051	1.024	1.067	1.027
$R_1{}^a$, $wR_2{}^b$	0.0325, 0.0773	0.0407, 0.1012	0.0324, 0.0823	0.0313, 0.0779	0.0411, 0.1042	0.0518, 0.1143

$^aR_1 = \Sigma||F_o|-|Fc||/\Sigma|F_o|$; $I_o > 2\sigma(I_o)$; $^bwR_2 = [\Sigma\, w(F_o^2-F_c^2)^2/\Sigma w(F_o^2)^2]^{1/2}$.

Table S3. Distances (in Å) for different types of interactions in **1b**, **2b**, **3b**, **4b**, **5b** and **6b**.

Interaction[i]	1b[ii]	2b[ii]	3b[ii]	4b[ii]	5b·DMF[ii]	6b[ii]
B···$H_{(CH2)}$	3.124 (**2**)	3.198 (**2**)	-	-	-	-
B···$H_{(pyr)}$	-	3.090 (**2**)	3.140 (**2**)	-	-	-
$C_{(ph)}$···$H_{(alkyne)}$	2.764 (**2**)	-	-	-	-	-
F···$H_{(pyr)}$	2.66 (**2**)	2.531-2.588 (**4**)	2.598-2.647 (**4**)	2.643-2.652 (**4**)	2.562 (**2**)	2.324 (**2**)
F···$H_{(ph)}$	2.526-2.605 (**4**)	2.599-2.625 (**4**)	2.514 (**2**)	2.397 (**2**)	2.544 (**2**)	-
F···$H_{(CH2)}$	2.546 (**2**)	2.547 (**2**)	-	2.544 (**2**)	-	-
F···$H_{(CH3)}$	-		-	-	2.643 (**2**)	-
F···$C_{(pyr)}$	-	3.056 (**2**)	-	-	3.145-3.167 (**4**)	-
F···$C_{(ph)}$	-	-	3.085 (**2**)	-	-	-
$_{(carboxy)}$C···$C_{(ph)}$	-	-	3.307 (**2**)	-	-	-
$_{(carboxy)}$C···$C_{(alkyne)}$	-	-	-	3.349 (**2**)	-	-
$_{(alkyne)}$C···$C_{(pyr)}$	-	-	-	3.342 (**2**)	-	-
$_{(alkyne)}$C···$O_{(carboxy)}$	-	-	-	3.144 (**2**)	-	-
$_{(carboxy)}$C···$H_{(carboxy)}$	-	-	-	2.799 (**2**)	-	2.680 (**2**)
$_{(pyr)}$C···$H_{(pyr)}$	-	-	-	-	2.861-2.881 (**4**)	2.763 (**1**)
$_{(sol)}$C···$H_{(carboxy)}$	-	-	-	-	2.525-2.585 (**2**)	-
$_{(carboxy)}$O···$O_{(carboxy)}$	-	-	-	-	-	2.651 (**2**)
$_{(sol)}$O···$O_{(carboxy)}$	-	-	-	-	2.539-2.546 (**2**)	-
$_{(pyr)}$H···$O_{(hydroxy)}$	2.592 (**2**)	-	2.702 (**2**)	-	-	-
$_{(pyr)}$H···$O_{(carboxy)}$	-	-	-	-	-	2.605-2.619 (**4**)
$_{(methyl)}$H···$O_{(carboxy)}$	-	-	-	-	2.695 (**2**)	-
$_{(carboxy)}$H···$O_{(carboxy)}$	-	-	-	-	-	1.836 (**2**)
$_{(carboxy)}$H···$O_{(sol)}$	-	-	-	-	1.731-2.656 (**3**)	-
$_{(ph)}$H···$O_{(carboxy)}$	-	-	-	-	2.497 (**2**)	-
$_{(ph)}$H···$O_{(sol)}$	-	-	-	-	2.528 (**2**)	-
$_{(alkyne)}$H···$O_{(carboxy)}$	-	-	-	2.237 (**2**)	-	-
$_{(pyr)}$H···$H_{(pyr)}$	-	-	-	2.075 (**2**)	2.307 (**1**)	2.224-2.324 (**2**)
$_{(pyr)}$H···$H_{(ph)}$	-	-	-	-	-	2.386 (**2**)
$_{(carboxy)}$H···$H_{(carboxy)}$	-	-	-	-	-	2.352 (**1**)

[i]Different types. [ii]Value in parenthesis gives the number of interactions present in the molecule.

Table S4. Photophysical properties of **1b-6b** in different solvents.

	Solvent	λ_{max}	λ_{em}	Stokes shift		Solvent	λ_{max}	λ_{em}	Stokes shift
1b	DMSO	501	516	580	**4b**	DMSO	504	525	794

ACCEPTED MANUSCRIPT

J. Porphyrins Phthalocyanines Downloaded from www.worldscientific.com
by UNIVERSITY OF NEW ENGLAND on 04/25/20. Re-use and distribution is strictly not permitted, except for Open Access articles.

	CH_3CN	495	509	556		CH3CN	499	517	698
	MeOH	496	511	592		MeOH	500	518	695
	THF	497	511	551		THF	502	521	726
	DCM	499	513	547		DCM	503	521	687
	Toluene	501	516	580		Toluene	506	527	788
2b	DMSO	502	522	763	**5b**	DMSO	506	531	930
	CH_3CN	497	514	665		CH_3CN	500	526	989
	MeOH	498	514	625		MeOH	502	526	909
	THF	501	517	618		THF	503	530	1013
	DCM	502	518	615		DCM	506	531	930
	Toluene	504	523	721		Toluene	507	535	1032
3b	DMSO	506	534	1036	**6b**	DMSO	504	527	866
	CH_3CN	501	527	985		CH_3CN	499	517	698
	MeOH	501	527	985		MeOH	500	517	658
	THF	504	530	973		THF	502	522	763
	DCM	505	529	898		DCM	502	523	800
	Toluene	507	535	1032		Toluene	506	527	788

Table S5. Calculated oscillator strength (f), excitation energy, wavelength, coefficient and its percentage contribution of transitions in ground state.

Compound	Excited State	Oscillator strength (f)	Excitation energy (eV)	Wavelength (nm)	Transition	Coefficient	% Contribution
1b	1	0.3751	2.9571	419.27	HOMO-2→LUMO	0.1592	5.1
					HOMO→LUMO	0.69051	95.3
					HOMO←LUMO	-0.10145	2.1
	2	0.232	3.2117	386.03	HOMO-1→LUMO	0.70187	98.5
	3	0.073	3.5432	349.93	HOMO-2→LUMO	0.68619	94.2
					HOMO→LUMO	-0.16227	5.3
	4	0.0379	3.748	330.8	HOMO-3→LUMO	0.70225	98.6
	5	0.004	3.991	310.66	HOMO-4→LUMO	0.69534	96.7
					HOMO-1→LUMO+1	-0.10623	2.3
2b	1	0.3752	2.9381	421.99	HOMO-2→LUMO	0.15797	4.9
					HOMO→LUMO	0.69026	95.3
					HOMO←LUMO	-0.10378	2.2
	2	0.0194	3.195	388.06	HOMO-1→LUMO	0.70032	98.1
	3	0.0814	3.5353	350.7	HOMO-2→LUMO	0.67987	92.4
					HOMO→LUMO	-0.16502	5.4
	4	0.0024	3.7023	334.88	HOMO-4→LUMO	0.5713	65.3
					HOMO-3→LUMO	-0.41145	33.9
	5	0.2032	3.788	327.31	HOMO-4→LUMO	0.40836	33.4

ACCEPTED MANUSCRIPT

J. Porphyrins Phthalocyanines Downloaded from www.worldscientific.com
by UNIVERSITY OF NEW ENGLAND on 04/25/20. Re-use and distribution is strictly not permitted, except for Open Access articles.

					HOMO-3→LUMO	0.5606	62.9
3b	1	0.3523	2.8902	428.98	HOMO-1→LUMO	0.15636	4.9
					HOMO→LUMO	0.6914	95.6
					HOMO←LUMO	-0.10253	2.1
	2	0.0555	3.4653	357.79	HOMO-1→LUMO	0.68033	92.6
					HOMO→LUMO	-0.15549	4.8
	3	0.0009	3.6598	338.77	HOMO-3→LUMO	0.63931	81.7
					HOMO-2→LUMO	0.2946	17.4
	4	0.3369	3.7628	329.5	HOMO-3→LUMO	-0.29139	16.9
					HOMO-2→LUMO	0.63246	80
	5	0.0646	3.8628	320.97	HOMO→LUMO+1	0.69524	96.7
	10	0.2136	4.8952	253.28	HOMO-2→LUMO+1	0.37511	28.1
					HOMO-8→LUMO	0.51328	52.7
					HOMO-7→LUMO	0.22089	9.8
					HOMO-4→LUMO+1	-0.10128	2.1
					HOMO→LUMO+4	0.10081	2
4b	1	0.3686	2.9333	422.68	HOMO-1→LUMO	-0.16655	5.5
					HOMO→LUMO	0.68926	95
					HOMO←LUMO	-0.10432	2.2
	2	0.0741	3.511	353.14	HOMO-1→LUMO	0.6826	93.2
					HOMO→LUMO	0.16873	5.7
	3	0.0004	3.6955	335.5	HOMO-3→LUMO	0.62165	77.3
					HOMO-2→LUMO	0.33094	21.9
	4	0.0239	3.7459	330.99	HOMO-3→LUMO	-0.16371	5.4
					HOMO-2→LUMO	0.25754	13.3
					HOMO→LUMO+1	0.63207	79.9
	5	0.2121	3.8044	325.89	HOMO-3→LUMO	-0.28357	16.1
					HOMO-2→LUMO	0.55812	62.3
					HOMO→LUMO+1	-0.30783	18.9
5b	1	0.3529	2.887	429.45	HOMO-1→LUMO	-0.1563	4.9
					HOMO→LUMO	0.69142	95.6
					HOMO←LUMO	-0.10257	2.1
	2	0.0553	3.4616	358.17	HOMO-1→LUMO	0.68012	92.5
					HOMO→LUMO	0.15513	4.8
					HOMO→LUMO+1	0.10157	2.1
		0.0002	3.6577	338.97	HOMO-3→LUMO	0.63624	80.9
					HOMO-2→LUMO	0.3017	18.2
	4	0.3038	3.7833	327.72	HOMO-3→LUMO	-0.2969	17.6
					HOMO-2→LUMO	0.63138	79.7

ACCEPTED MANUSCRIPT

J. Porphyrins Phthalocyanines Downloaded from www.worldscientific.com
by UNIVERSITY OF NEW ENGLAND on 04/25/20. Re-use and distribution is strictly not permitted, except for Open Access articles.

	5	0.0671	3.8566	321.48	HOMO→LUMO+1	0.6954	96.7
6b	1	0.3718	2.9304	423.1	HOMO-1→LUMO	0.16634	5.5
					HOMO→LUMO	0.68937	95
					HOMO←LUMO	-0.10458	2.2
	2	0.0729	3.5057	353.66	HOMO-1→LUMO	0.68133	92.8
					HOMO→LUMO	-0.16776	5.6
	3	0.0016	3.6934	335.69	HOMO-3→LUMO	-0.374	27.9
					HOMO-2→LUMO	0.59496	70.8
	4	0.0096	3.706	334.55	HOMO-2→LUMO	0.10966	2.4
					HOMO→LUMO+1	0.68848	94.8
	5	0.235	3.8403	322.85	HOMO-3→LUMO	0.58265	67.9
					HOMO-2→LUMO	0.35888	25.8
					HOMO→LUMO+1	-0.12879	3.3

Table S6. Oscillator strength (f), excitation energy, wavelength, coefficient and its percentage contribution of transitions in transition state.

Compound	Excited State	Oscillator strength (f)	Excitation energy (eV)	Wavelength (nm)	Transition	Coefficient of transition	% contribution
1b	1	0.4001	2.9979	413.58	HOMO-2→LUMO	0.15947	5.1
					HOMO→LUMO	0.68673	94.3
					HOMO←LUMO	-0.10552	2.2
	2	0.0026	3.055	405.84	HOMO-1→LUMO	0.70122	98.3
	3		3.5858	345.76	HOMO-2→LUMO	0.68584	94.0
					HOMO→LUMO	-0.16587	5.5
	4	0.0269	3.7911	327.04	HOMO-3→LUMO	0.70275	98.8
	5	0.0249	3.9398	314.7	HOMO-4→LUMO	0.70194	98.5
2b	1	0.3023	2.9529	419.88	HOMO-2→LUMO	0.12913	3.3
					HOMO-1→LUMO	-0.25118	12.6
					HOMO→LUMO	0.64878	84.2
	2	0.0932	3.1217	397.17	HOMO-2→LUMO	0.11054	2.4
					HOMO-1→LUMO	0.65451	85.7
					HOMO→LUMO	0.23115	10.7
	3	0.0778	3.5913	345.23	HOMO-2→LUMO	0.68247	93.6
					HOMO→LUMO	-0.15819	5.0
	4	0.0274	3.786	327.48	HOMO-4→LUMO	0.70279	98.8
	5	0.0305	3.7973	326.51	HOMO-3→LUMO	0.69566	96.8
3b	1	0.3996	2.9902	414.63	HOMO-1→LUMO	-0.16973	5.7
					HOMO→LUMO	0.68733	94.5

ACCEPTED MANUSCRIPT

J. Porphyrins Phthalocyanines Downloaded from www.worldscientific.com
by UNIVERSITY OF NEW ENGLAND on 04/25/20. Re-use and distribution is strictly not permitted, except for Open Access articles.

					HOMO←LUMO	-0.1071	2.3
	2	0.0847	3.5711	347.19	HOMO-1→LUMO	0.68392	93.5
					HOMO→LUMO	0.17435	6.1
	3	0.0275	3.7651	329.29	HOMO-3→LUMO	0.70275	98.7
	4	0.001	3.7919	326.97	HOMO-5→LUMO	-0.14271	4.1
					HOMO-2→LUMO	0.67722	91.7
	5	0.0005	3.9547	313.51	HOMO→LUMO+1	0.70237	98.7
4b	1	0.4001	2.9906	414.58	HOMO-1→LUMO	0.17358	6.0
					HOMO→LUMO	0.68667	94.3
					HOMO←LUMO	-0.10656	2.3
	2	0.0906	3.5782	346.5	HOMO-1→LUMO	0.68329	93.4
					HOMO→LUMO	-0.17763	6.3
	3	0.0009	3.7642	329.37	HOMO-2→LUMO	0.52547	55.2
					HOMO→LUMO+1	-0.46911	44.0
	4	0.0519	3.7821	327.82	HOMO-2→LUMO	0.46659	43.5
					HOMO→LUMO+1	0.5264	55.4
	5	0.0007	3.841	322.79	HOMO-3→LUMO	0.69347	96.2
5b	1	0.405	2.9907	414.57	HOMO-1→LUMO	0.16971	5.7
					HOMO→LUMO	0.68716	94.4
					HOMO←LUMO	-0.10678	2.3
	2	0.0861	3.5714	347.16	HOMO-1→LUMO	0.68435	93.7
	3	0.0273	3.7693	328.93	HOMO→LUMO	-0.17384	6.0
					HOMO-2→LUMO	0.70253	98.7
	4	0.0003	3.782	327.83	HOMO→LUMO+1	0.7036	99.0
	5	0.0005	3.8665	320.67	HOMO-4→LUMO	-0.20805	8.7
					HOMO-3→LUMO	0.67116	90.1
6b	1	0.4033	2.9902	414.64	HOMO-1→LUMO	0.17427	6.1
					HOMO→LUMO	0.68659	94.3
					HOMO←LUMO	-0.10663	2.3
	2	0.0926	3.5777	346.54	HOMO-1→LUMO	0.68314	93.3
					HOMO→LUMO	-0.17829	6.4
	3	0.0006	3.7583	329.9	HOMO-2→LUMO	-0.41396	34.3
					HOMO→LUMO+1	0.57061	65.1
	4	0.048	3.7772	328.24	HOMO-2→LUMO	0.56787	64.5
					HOMO→LUMO+1	0.41438	34.6
	5	0.0006	3.8602	321.19	HOMO-4→LUMO	-0.14354	4.1
					HOMO-3→LUMO	0.68852	94.8

ACCEPTED MANUSCRIPT

J. Porphyrins Phthalocyanines Downloaded from www.worldscientific.com
by UNIVERSITY OF NEW ENGLAND on 04/25/20. Re-use and distribution is strictly not permitted, except for Open Access articles.

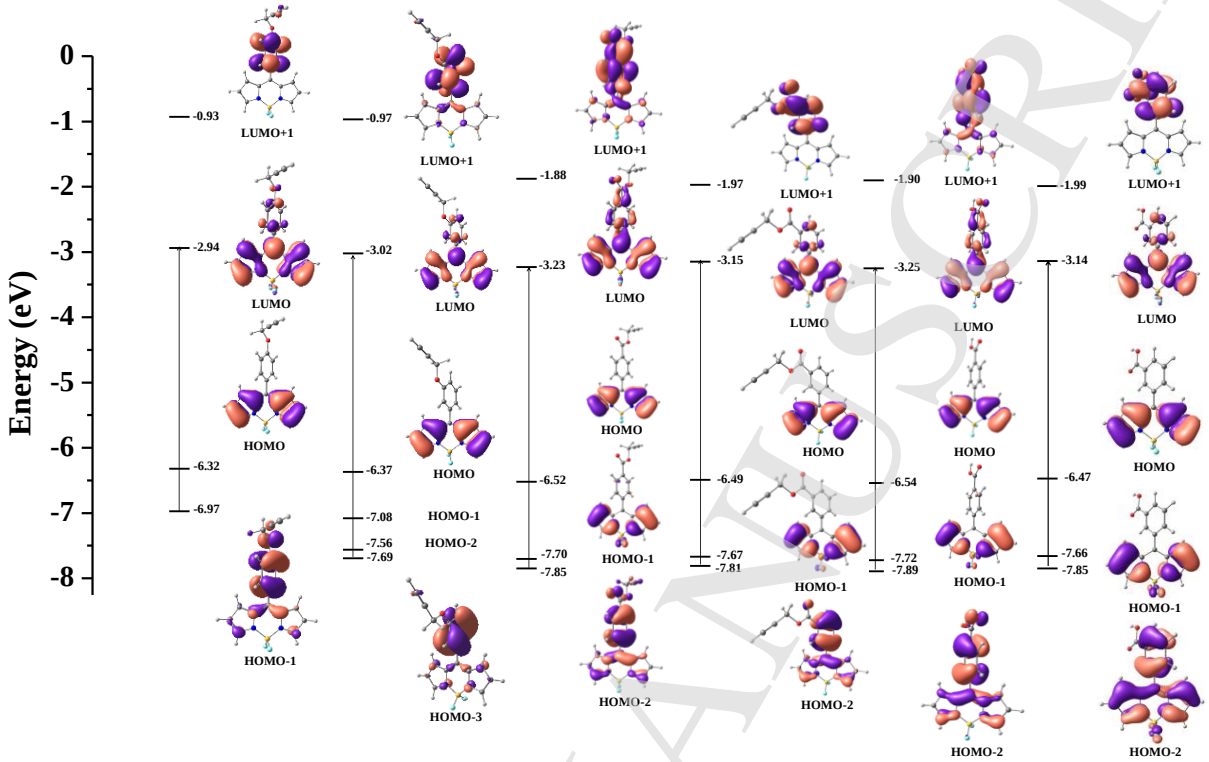

Table S7. Log (quantum yield) *versus* log (viscosity)

Compound	log(ϕ_f)	log (η)	Compound	log(φ_f)	log (η)
1b	0.88081	-1.69937	**4b**	0.38021	-2.06534
	1.59106	-1.53023		0.88081	-1.82344
	2.03342	-1.3162		1.59106	-1.48372
	2.38202	-1.14336		2.03342	-1.07567
	2.82217	-0.94755		2.38202	-0.92176
	3.16346	-0.67301		2.82217	-0.75004
2b	0.38021	-2.26889	**5b**	0.38021	-2.59561
	0.88081	-2.10787		0.88081	-2.42404
	1.59106	-1.9028		1.59106	-1.94723
	2.03342	-1.49892		2.03342	-1.75721
	2.38202	-1.29976		2.38202	-1.57019
	2.82217	-1.09815		2.82217	-1.32353
	3.16346	-0.80063		3.16346	-1.27383
3b	0.38021	-2.34574	**6b**	0.38021	-2.22692
	0.88081	-2.1012		0.88081	-2.15304
	1.59106	-1.55554		1.59106	-1.84531
	2.03342	-1.39703		2.03342	-1.51987
	2.38202	-1.26403		2.38202	-1.33772
	2.82217	-0.86469		2.82217	-1.17292
	3.16346	-0.59497		3.16346	-1.05875

ACCEPTED MANUSCRIPT

Table S8. Molar extinction coefficient and quantum yield of compounds, **1b-6b** at 1 x 10^{-7} M in ethanol, λ_{ex} = 480 nm. Fluorescence quantum yields (Φ_f) were calculated using fluorescein in aqueous NaOH (0.1 N, Φ_f = 0.90) at λ_{ex}= 480 nm and slit width, 10.

Compound	Φ_f	log ε
1b	0.05	4.32
2b	0.04	4.67
3b	0.01	4.70
4b	0.03	4.91
5b	0.02	3.91
6b	0.05	4.47

J. Porphyrins Phthalocyanines Downloaded from www.worldscientific.com
by UNIVERSITY OF NEW ENGLAND on 04/25/20. Re-use and distribution is strictly not permitted, except for Open Access articles.

ACCEPTED MANUSCRIPT